Isohelicity and Strand Selectivity in the Minor Groove Binding of Chiral (1*R*,2*R*)- and (1*S*,2*S*)-Bis(netropsin)-1,2-cyclopropanedicarboxamide Ligands to Duplex DNA

Malvinder P. Singh,† Bertrand Plouvier,† G. Craig Hill,§ Juergen Gueck,†,‡ Richard T. Pon,⊥ and J. William Lown*,†

Contribution from the Department of Chemistry, University of Alberta, Edmonton, Alberta T6G 2G2, Canada, Xavier College of Pharmacy, New Orleans, Lousiana, and Regional DNA Synthesis Laboratory, University of Calgary, Calgary, Alberta, Canada

Received May 20, 1993. Revised Manuscript Received February 4, 1994®

Abstract: The sequence-selective DNA binding within the minor groove of four base pairs long AT rich segments for the naturally occurring oligopyrrolecarboxamides, netropsin and distamycin, have been characterized by NMR and X-ray techniques which provide valuable information on the factors for specific molecular recognition and binding efficiency. A special interest in developing longer dimeric bis-netropsin and bis-distamycin compounds arises from their potential applications as gene control agents targeted against larger DNA segments in a sequence specific manner. Herein we describe the use of fixed C_2-symmetric dimeric arrangements of netropsin segments, in opposing orientations and joined through optically pure cyclopropane-1,2-dicarboxamide templates, to "extend the code" for isohelical and chiral recognition of eight AT base pairs long minor groove in a right-handed B-DNA fragment. The structural analysis of the diastereomeric complex formed between d(CGAAAATTTTCG)$_2$ and (−)-(1*R*,2*R*)-bis(netropsin)-1,2-cyclopropanedicarboxamide (BNC), and of that between the same DNA fragment and the enantiomeric (+)-(1*S*,2*S*)-BNC ligand, was performed by one- and two-dimensional NMR methods. These results indicate a perfectly matching isohelical and strand specific binding for (1*R*,2*R*)-BNC where each of the two netropsin subunits is oriented against a 5′-TTTT site. The cyclopropane linker and the *N*-methylpyrrole rings follow the natural right-handed twist of the base pairs along the minor groove of the 5′-AAAATTTT segment, and the complex is stabilized by single linear hydrogen bonds with the thymidine O2 atoms, instead of the three-center bifurcated bonds proposed for the binding of netropsin to alternating AT segments. The relative orientation of the cyclopropane group (with its methylene projected away from the DNA) for the (1*S*,2*S*)-BNC enantiomer is the same as observed for (1*R*,2*R*)-BNC which forces each netropsin subunit to be aligned differently in a less favorable arrangement (against 5′-AAAA sites). Binding in this case therefore induces a further twist of the planar amide groups and two *N*-methylpyrrole ring systems in each of the netropsin subunits. The twisting is detected by NOE interactions and, in contrast with the situation for (1*R*,2*R*)-BNC, is attributed to the adjustments that are required by the inherent affinity for hydrogen-bonding by the amide NHs of (1*S*,2*S*)-BNC to the continguous arrangement of thymidine O2 atoms on the complementary strand.

Introduction

Design and development of sequence-specific DNA binding agents is being actively pursued for applications as probes in molecular biology and as drugs for genetic targeting.[1,2] Minor groove binders such as distamycin and netropsin (Figure 1a), two members of the pyrrole-amidinium class of antibiotics, are oligomeric *N*-methylpyrrolecarboxamide peptides, which exhibit a pronounced selectivity for the minor groove of AT-rich sites in double stranded DNA.[3,4] Their stable noncovalent complexes with DNA fragments containing (AATT)$_2$, (ATAT)$_2$, and (AAATTT)$_2$ sites have been structurally characterized by solution NMR[5] and X-ray crystallography[6] to define the location, orientation, and minimum binding site size of 4–5 continguous AT base pairs. The structural characteristics, in conjunction with molecular interaction studies, reviewed elsewhere,[1a,d,i,3] indicate several factors that contribute favorably to the stability of these ligand–DNA complexes: (i) hydrogen bonding between the amide NHs of the oligopeptide ligands and thymine O2 and

* To whom correspondence should be addressed. Tel (403) 492-3646.
† University of Alberta.
‡ Present address: Lonza AG, CH-3930 Visp (VS), Switzerland.
§ Xavier College of Pharmacy.
⊥ University of Calgary.
® Abstract published in *Advance ACS Abstracts*, July 1, 1994.

(1) For leading reviews on DNA binding ligands, see: (a) Dervan, P. B. *Science (Washington, DC)* **1986**, *232*, 464–471. (b) Barton, J. K. *Science (Washington, DC)* **1986**, *233*, 727–734. (c) Hurley, L. H.; Boyd, F. L. *Annu. Rep. Med. Chem.* **1987**, *22*, 259–268. (d) Pullman, B. *Adv. Drug. Res* **1989**, *18*, 1–113. (e) Lown, J. W. In *Molecular Basis of Specificity in Nucleic Acid·Drug Interactions*; Pullman, B., Jortner, J., Eds.; Kluwer Acad. Publishers: Dordrecht, Netherlands, 1990; pp 103–122. (f) Nielsen, P. E. *Bioconjugate Chem.* **1991**, *2*, 1–12. (g) Bailly, C.; Hénichart, J. P. *Bioconjugate Chem.* **1991**, *2*, 379–393. (h) Lown, J. W. *Antiviral Res.* **1992**, *17*, 179–196. (i) Singh, M. P.; Lown, J. W. In *Studies in Medicinal Chemistry*, Atta·ur·Rahman, Ed., Harwood Acad. Publishers: Amsterdam, in press.

(2) For an overview of antisense and triplex-forming oligonucleotides, see: (a) Moser, H. E.; Dervan, P. B. *Science (Washington, DC)* **1987**, *238*, 645–650. (b) Cooney, M.; Czernuszewicz, G.; Postel, E. H.; Flint, S. J.; Hogan, M. E. *Science (Washington, DC)* **1988**, *241*, 456–459. (c) A Monograph on *Oligodeoxynucleotides: Antisense inhibitors of gene expression*; *Topics in Molecular and Structural Biology*; Cohen, J. S., Ed.; MacMillan Press: London, 1989; Vol. 12. (d) Uhlmann, E.; Peyman, A. *Chem. Rev.* **1990**, *90*, 543–584. (e) Helène, C. *Anti·Cancer Drug Des.* **1991**, *6*, 569–584. (f) Thuong, N. T.; Helène, C. *Angew. Chem., Int. Ed. Engl.* **1993**, *32*, 666–690.

(3) (a) Hahn, F. E. In *Antibiotics III. Mechanism of Action of Antimicrobial and Antitumor Agents*; Corcoran, J. W., Hahn, F. E., Eds.; Springer-Verlag: New York, 1975; p 79. (b) Zimmer, C.; Wahnert, U. *Prog. Biophys. Mol. Biol.* **1986**, *47*, 31–112.

(4) The AT-sequence selectivity exhibited by netropsin and distamycin is matched only by a few synthetic agents; for a few selected examples, see: *Hoechst 33258* (a) Pjura, P. E.; Grzeskowiak, K.; Dickerson, R. E. *J. Mol. Biol.* **1987**, *197*, 257–271. (b) Teng, M.·K.; Usman, N.; Frederick, C. A.; Wang, A. H.·J. *Nucleic Acids Res.* **1988**, *16*, 2671–2690. *Berenil* (c) Brown, D. G.; Sanderson, M. R.; Skelly, J. V.; Jenkins, T. C.; Brown, T.; Garman, E.; Stuart, D. I.; Neidle, S. *EMBO J.* **1990**, *9*, 1329–1334. *DAPI* (d) Larsen, T. A.; Goodsell, D. S.; Cascio, D.; Grzeskowiak, K.; Dickerson, R. E. *J. Biomol. Struct. Dyn.* **1989**, *7*, 447–491. *SN6999* (e) Leupin, W.; Chazin, W. J.; Hyberts, S.; Denny, W. A.; Wüthrich, K. *Biochemistry* **1986**, *25*, 5902–5910.

0002-7863/94/1516-7006$04.50/0

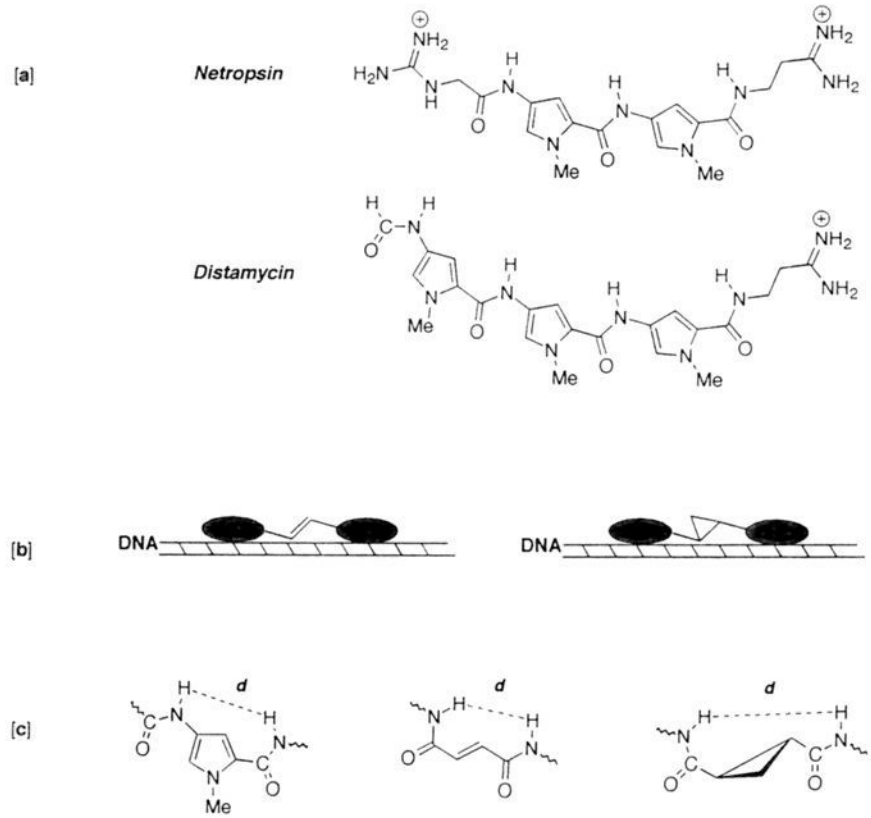

Figure 1. (a) Structural formulas of netropsin and distamycin, (b) the general schematic representations of bidentate DNA complexation of dimeric ligands linked by rigid olefinic or cyclopropane groups. Filled ellipses correspond to the DNA binding oligo(*N*-methylpyrrolecarboxamide) frameworks, and (c) illustration of the general similarities for the repeat distances *d* between *N*-methylpyrrolecarboxamide repeat units of netropsin and distamycin with those for geometrically constrained *trans*-olefenic and conformationally constrained *trans*-cyclopropane dicarboxamides.

adenine N3 atoms; (ii) an overall shape complementarity as a result of close intermolecular van der Waals contacts between the ligand and the walls of the minor groove in addition to those with the glycosidic H1′ and adenine H2 protons; and (iii) electrostatic interactions between the positively charged end-groups in the ligands and the polyanionic DNA and/or a highly negative potential at the AT-rich minor groove presumably provide the initial attraction. In addition, an unfavorable binding of these agents to GC-containing sequences arises due to a steric clash between the guanine amino group at the floor of the minor groove and the pyrrole H3 protons of the ligands.

Lexitropsins are rationally designed synthetic analogs of netropsin/distamycin where G·C base-pair recognizing elements have been judiciously incorporated to alter the DNA sequence selectivity.[7] For example, replacement of *N*-methylpyrrole units with other five-membered heterocycle rings to provide additional hydrogen-bond acceptor sites, and modifications in the side-chain residues to change the electrostatic components, has led to the development of novel derivatives with varying degrees of G·C base pair acceptance in contrast to the strick affinity of the parent compounds for AT-rich segments in DNA.

A related goal toward the development of new sequence specific DNA binding molecules is the design of molecular vectors with particular relevance to their improved selective biological potency. One obvious argument with respect to this strategy is that compounds bearing a larger number of DNA recognizing subunits (e.g., pyrrolecarboxamide in the case of netropsin and distamycin and benzimidazole in Hoechst 33258) would have a larger binding site size and consequently a better potential for binding more strongly to, and discriminating between, defined DNA sequences.[1a,e] Previous studies by Dervan's group, carried out on extended oligopyrrolecarboxamide analogs of distamycin, where the number of individual carboxamide subunits was varied from 4–7, have shown partial success toward this end of building synthetic oligopeptides that recognize and bind to larger (5–8 base pairs long) contiguous AT segments of double helical DNA.[8] However, structural details on the DNA complexes of these larger

(5) For previous ^{1}H-NMR studies on 1:1 DNA complexes of netropsin and distamycin: (a) Patel, D. J. *Proc. Natl. Acad. Sci. U.S.A.* **1982**, *79*, 6424–6428. (b) Patel, D. J.; Shapiro, L. *Biochimie* **1985**, *67*, 887–915. (c) Sarma, M. H.; Gupta, G.; Sarma, R. H. *J. Biomol. Struct. Dyn.* **1985**, *2*, 1085–1095. (d) Patel, D. J.; Shapiro, L. *J. Biol. Chem.* **1986**, *261*, 1230–1239. (e) Klevit, R. E.; Wemmer, D. E.; Reid, B. R. *Biochemistry* **1986**, *25*, 3296–3303. (f) Pelton, J. G.; Wemmer, D. E. *Biochemistry* **1988**, *27*, 8088–8096. For those on closely related structures: (g) Sarma, M. H.; Gupta, G.; Garcia, A. E.; Umemoto, K.; Sarma, R. H. *Biochemistry* **1990**, *29*, 4723–4734. (h) Conte, M. R.; Fattorusso, E.; Paloma, L. G.; Mayol, L. *Bioorg. Med. Chem. Lett.* **1992**, *2*, 1299–1304.

(6) Crystal structures on both netropsin and distamycin complexed with AT-rich sites of several DNA fragments are reported: (a) Berman, H. M.; Neidle, S.; Zimmer, C.; Thrum, H. *Biochim. Biophys. Acta* **1979**, *561*, 124–131. (b) Kopka, M. L.; Yoon, C.; Goodsell, D.; Pjura, P.; Dickerson, R. E. *Proc. Natl. Acad. Sci. U.S.A.* **1985**, *82*, 1376–1380. (c) Kopka, M. L.; Yoon, C.; Goodsell, D.; Pjura, P.; Dickerson, R. E. *J. Mol. Biol.* **1985**, *183*, 553–563. (d) Kopka, M. K.; Pjura, P.; Yoon, C.; Goodsell, D.; Dickerson, R. E. In *Structure and Motion: Membranes, Nucleic Acids, and Proteins*; Clementi, E., Corongiu, G., Sarma, M. H., Sarma, R. H., Eds.; Adenine Press: New York; 1985; pp 461–483. (e) Coll, M.; Frederick, C. A.; Wang, A. H.-J.; Rich, A. *Proc. Natl. Acad. Sci. U.S.A.* **1987**, *84*, 8385–8389. (f) Coll, M.; Aymami, J.; van der Marel, G. A.; van Boom, J. H.; Rich, A.; Wang, A. H.-J. *Biochemistry* **1989**, *28*, 310–320. (g) Wang, A. H.-J.; Teng, M.-K. In *Crystallographic and Modeling Methods in Molecular Design*; Bugg, C. E., Ealick, S. E., Eds.; Springer-Verlag: New York, 1990; pp 123–150. (h) Sriram, M.; van der Marel, G. A.; Roelen, H. L. P. F.; van Boom, J. H.; Wang, A. H.-J. *Biochemistry* **1992**, *31*, 11823–11834. (i) Tabernero, L.; Verdaguer, N.; Coll, M.; Fita, I.; van der Marel, G. A.; van Boom, J. H.; Rich, A.; Aymami, J. *Biochemistry* **1993**, *32*, 8403–8410.

(7) (a) Lown, J. W.; Krowicki, K.; Bhat, U. G.; Skorobogaty, A.; Ward, B.; Dabrowiak, J. C. *Biochemistry* **1986**, *25*, 7408–7416. (b) Wade, W. S.; Dervan, P. B. *J. Am. Chem. Soc.* **1987**, *109*, 1574–1575. (c) Lee, M.; Krowicki, K.; Hartley, J. A.; Pon, R. T.; Lown, J. W. *J. Am. Chem. Soc.* **1988**, *110*, 3641–3649. Extensive accounts on GC-base-pair binding specificity by lexitropsins are reviewed in the following: (d) Lown, J. W. *Anti-Cancer Drug Des.* **1988**, *3*, 25–40. (e) Kopka, M. L.; Larsen, T. A. In *Nucleic Acid Targeted Drug Design*; Propst, C. L., Perun, T. L., Eds.; Marcel Dekker: New York; 1992; pp 303–374. (f) Lown, J. W. *Chemtracts-Org. Chem.* **1993**, *6*, 205–237.

oligopeptides are not available yet, and it remains to be seen if the higher number of *N*-methylpyrrolecarboxamide subunits also twist in a screw sense to match the natural twist of the right-handed DNA helix. The observation that GC base pairs frequently appear in the most preferred binding sites of these higher oligopeptide homologs and that their binding constants have been significantly less than the values anticipated suggests that not every pyrrolecarboxamide subunit is able to make similar favorable contacts with the DNA minor groove in the bound state.[1a,8b] This is not surprising since theoretical considerations and isohelical analysis showed that the repeating pyrrolecarboxamide unit is about 20% longer than is required to match perfectly the base pair rise along the minor groove of the DNA helix.[9]

Design Rationale and Experimental Strategy. From a design perspective, an alternative approach to developing molecules capable of binding long DNA sequences therefore is to overcome this problem of a lack of phasing or spatial correspondence between repeat units in the ligand and the DNA receptor. This reasoning led us,[10] and others,[11,12] to couple two high-affinity and highly selective DNA binding units via linker groups so that both can bind to DNA simultaneously (Figure 1). The use of various groups for linking two netropsin/distamycin units is described in our earlier studies which show that conformationally constrained cycloalkane and olefinic linkers proved more effective (in *trans* configuration) for the desired high-affinity bidentate binding of dimeric oligopeptides to duplex DNA[10c] than flexible polymethylene chain where both the mono- and bidentate binding modes prevail.[10b]

The use of fairly detailed molecular mechanics calculations for probing ideal characteristics of the linker functionality was also reported in an earlier study to show the importance of structural, stereochemical, and conformational aspects.[10c] The right-handedness of double stranded DNA helix makes it a chiral receptor so that the chirality of designed minor groove binding ligands is also anticipated to influence binding characteristics. However, only a limited number of studies are reported on this aspect in the case of minor groove binding agents, e.g., a comparison of optically pure enantiomers of naturally occurring antibiotics anthelvencin and dihydrokikumycin[13] and footprinting analyses on synthetic bis-netropsin analogs employing enantiomeric dihydroxysuccinic acid linker groups.[14]

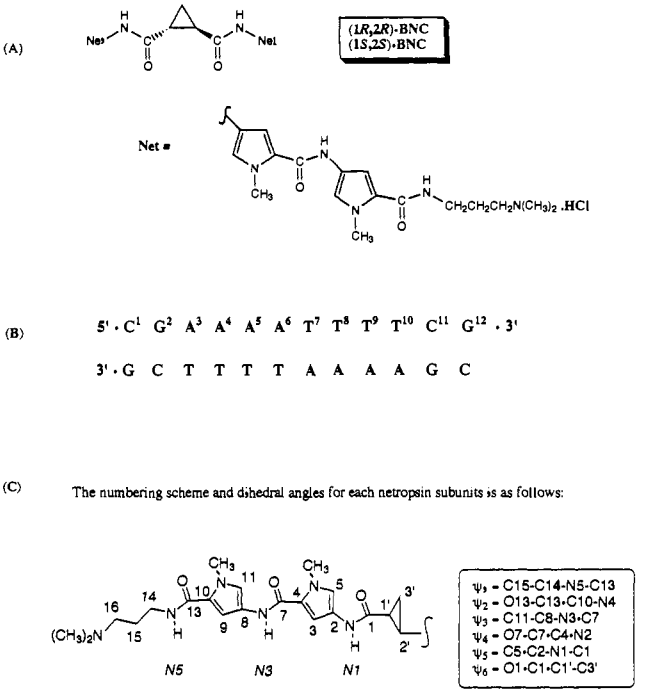

Figure 2. (a) Structures for the optically pure enantiomers of BNC, (1*R*,2*R*)- and (1*S*,2*S*)-bis(netropsin)-1,2-cyclopropanedicarboxamide and (b) the duplex dodecaribodeoxynucleotide sequence used in the present NMR analyses. Also shown is (c) the numbering scheme dihedral angles defined for each of the symmetric bis(*N*-methylpyrrolecarboxamide) subunits of the BNC ligands.

In order to obtain structural information and further insights on chiral discrimination in the binding of optically active minor groove binding ligands, we report, in this study, a constrained system of dimeric DNA-binding netropsin motifs (BNC) using optically pure C_2-symmetric linkers, (1*R*,2*R*)- and (1*S*,2*S*)-*trans*-1,2-cyclopropanedicarboxamide [see Figure 2 for structures and nomenclature].

We have used a dodecamer DNA fragment for investigating solution structures by employing NMR methods to analyze the ligand-DNA interactions. The search for distance-dependent intermolecular NOE interactions is vital in these studies for determining the binding location and site size together with the stereochemical orientation of small molecular weight ligands on appropriately selected DNA fragments.[4] This approach has enabled us to make direct comparison of two ligands containing identical binding domains in each half and differing in the absolute configuration of the central cyclopropane linker template.

The self-complementary DNA fragment d-(CGAAAAT-TTTCG)$_2$ containing eight AT base pairs was selected for this purpose, with one central 5'-AAAA-3' stretch on each strand as potential sites for a bidentate association of the netropsin arms, and two C·G base pairs at each end to diminish end-fraying of the double stranded helix (Figure 2). In the two ligands, the central cyclopropane linker contains amide NHs on either side and closely matches the *N*-methylpyrrolecarboxamide DNA-binding unit[1a,e] in terms of shape, curvature, and disposition of amide NHs so that the dimeric BNC ligands are like hexamides which, according to the general empirical rule of $n + 1$ base pairs required for binding to n amides, would optimally bind to a 7–8 base pairs long segment.[1a,8] Additional data from previous binding studies[3b,15a,b] suggest that neotropsin exhibits an entropy-driven preferential sequence specificity for the minor groove of poly-

(8) (a) Schultz, P. G.; Dervan, P. B. *J. Biomol. Struct. Dyn.* **1984**, *1*, 1133–1147. (b) Youngquist, R. S.; Dervan, P. B. *Proc. Natl. Acad. Sci. U.S.A.* **1985**, *82*, 2565–2569.

(9) Goodsell, D.; Dickerson, R. E. *J. Med. Chem.* **1986**, *29*, 727–733.

(10) (a) Lown, J. W.; Krowicki, K.; Balzarini, J.; Newman, R. A.; De Clercq, E. *J. Med. Chem.* **1989**, *32*, 2368–2375. (b) Kissinger, K. L.; Dabrowiak, J. C.; Lown, J. W. *Chem. Res. Toxicol.* **1990**, *3*, 162–168. (c) Rao, K. E.; Zimmermann, J.; Lown, J. W. *J. Org. Chem.* **1991**, *56*, 786–797. (d) Rao, K. E.; Krowicki, K.; Balzarini, J.; De Clercq, E.; Newman, R. A.; Lown, J. W. *Actual. Chim. Ther.* **1991**, *18*, 21–42. (e) Wang, W.; Lown, J. W. *J. Med. Chem.* **1992**, *35*, 2890–2897.

(11) (a) Schultz, P. G.; Dervan, P. B. *J. Am. Chem. Soc.* **1983**, *105*, 7748–7750. (b) Schultz, P. G.; Dervan, P. B. *Proc. Natl. Acad. Sci. U.S.A.* **1983**, *80*, 6834–6837. (c) Youngquist, R. S.; Dervan, P. B. *J. Am. Chem. Soc.* **1985**, *107*, 5528–5529. (d) Griffin, J. H.; Dervan, P. B. *J. Am. Chem. Soc.* **1987**, *109*, 6840–6842. (e) Youngquist, R. S.; Dervan, P. B. *J. Am. Chem. Soc.* **1987**, *109*, 7564–7566. (f) Wang, A. H.-J.; Cottens, S.; Dervan, P. B.; Yesinowski, J. P.; van der Marel, G. A.; van Boom, J. H. *J. Biomol. Struct. Dyn.* **1989**, *7*, 101–117.

(12) (a) Khorlin, A. A.; Krylov, A. S.; Grokhovsky, S. L.; Zhuzhe, A. L.; Zasadatelev, A. S.; Gursky, G. V.; Gottikh, B. P. *FEBS Lett.* **1980**, *118*, 311–314. (b) Gursky, G. V.; Zasadatelev, A. S.; Zhuzhe, A. L.; Khorlin, A. A.; Grokhovsky, S. L.; Streltsov, S. A.; Surovaya, A. N.; Nikitin, S. M.; Krylov, A. S.; Retchinsky, V. O.; Michailov, M. V.; Beabealashvili, R. S.; Gottikh, B. P. *Cold Spring Harbor Symp. Quant. Biol.* **1982**, *47*, 367–378. (c) Leinsoo, T. A.; Nikolaev, V. A.; Grokhovskii, S. L.; Surovaya, A. M.; Sidorova, N. Y.; Strel'tsov, S. A.; Zasedatelev, A. S.; Zhuzhe, A. L.; Gurskii, G. V. *Molek. Biol. (USSR)* **1989**, *23*, 1616–1637.

(13) Anthelvencin and dihydrokikumycin are two chiral members of the pyrrole·amidine class of naturally occurring compounds that includes netropsin and distamycin: (a) Lee, M.; Shea, R. G.; Hartley, J. A.; Kissinger, K.; Pon, R. T.; Vesnaver, G.; Breslauer, K. J.; Dabrowiak, J. C.; Lown, J. W. *J. Am. Chem. Soc.* **1989**, *111*, 345–354. (b) Lee, M.; Shea, R. G.; Hartley, J. A.; Lown, J. W.; Kissinger, K.; Dabrowiak, J. C.; Vesnaver, G.; Breslauer, K. J.; Pon, R. T. *J. Mol. Recogn.* **1989**, *2*, 6–17.

(14) Griffin, J. H.; Dervan, P. B. *J. Am. Chem. Soc.* **1986**, *108*, 5008–5009.

(15) (a) Marky, L. A.; Breslauer, K. J. *Proc. Natl. Acad. Sci. U.S.A.* **1987**, *84*, 4359–4363. (b) Marky, L. A.; Kupke, K. J. *Biochemistry* **1989**, *28*, 9982–9988. (c) Wade, W. S.; Mrksich, M.; Dervan, P. B. *J. Am. Chem. Soc.* **1992**, *114*, 8783–8794. (d) Wade, W. S.; Mrksich, M.; Dervan, P. B. *Biochemistry* **1993**, *32*, 11385–11389.

Scheme 1. Stereoselective Syntheses of Optically Pure (1*R*,2*R*)- and (1*S*,2*S*)-BNC Ligands

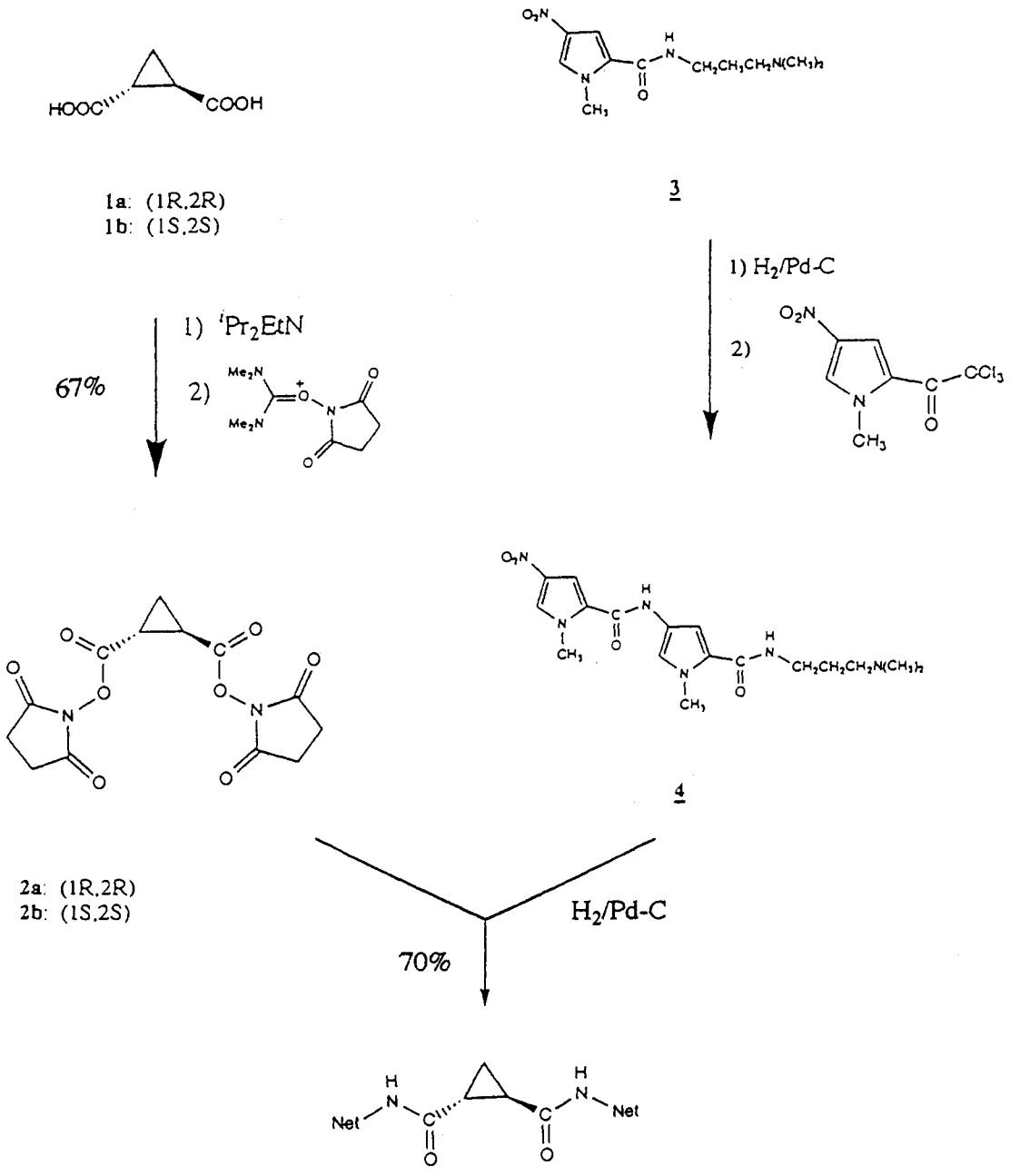

(dA)·poly(dT) compared with a predominantly enthalpy-driven binding to the alternating poly(dA-dT) copolymer with a lower affinity; hence studies were performed on a duplex DNA containing a 5′-AAAA-3′ (*vis a vis* the complementary TTTT) segment. In the case of distamycin-like tripeptide analogs, a strict preference for binding to TTTTT sites has been explicitly demonstrated only recently in a comparison of quantitative footprinting data for TTTTT, AATAA, and TTATT sites.[15c,d]

Synthesis. Our syntheses of chiral dimeric bis-netropsin analogs (−)-(1*R*,2*R*)-BNC and (+)-(1*S*,2*S*)-BNC utilizes a highly convergent approach as outlined in Scheme 1. The required starting material **3** containing one pyrrole unit was prepared following a reported procedure[16a] and further elaborated to the bispyrrole derivative **4** via reduction of the nitro group and condensation with *N*-methyl-2-trichloroacetyl-4-nitropyrrole.[16] Optically pure enantiomers of *trans*-1,2-cyclopropanedicarboxylic acid were prepared according to the method of Yamamoto.[17] Activation of the diacids in the form of bis(*N*-succinimidyl)-diesters[18] **2a** and **2b** was followed individually by condensation with the same bispyrrole amine, obtained by hydrogenation of **4**, to afford enantiomers (1*R*,2*R*)-BNC and (1*S*,2*S*)-BNC, respectively, in optically pure forms.

Experimental Section

In the procedures described below, all the reactions were carried out under N_2 atmosphere and the evaporations were performed in vacuo

(16) (a) Nishiwaki, E.; Tanaka, S.; Lee, H.; Shibuya, M. *Heterocycles* **1988**, *27*, 1945–1952. (b) Lown, J. W. *Org. Prep. Proceed. Intl.* **1989**, *21*, 1–46, and references cited therein.

(17) (a) Misumi, A.; Iwanaga, K.; Furuta, K.; Yamamoto, H. *J. Am. Chem. Soc.* **1985**, *107*, 3343–3345. (b) Furuta, K.; Iwanaga, K.; Yamamoto, H. *Org. Synth.* **1989**, *67*, 76–83.

using rotary evaporator. All starting organic chemicals were obtained from Aldrich Chemical Co., unless otherwise indicated, and were used without further purifications. HPLC grade solvents were used for chromatography. Anhydrous DMF was distilled under reduced pressure from CaH_2. Melting points were recorded on a Fisher-Johns capillary apparatus and are uncorrected. The ^1H NMR spectra for characterizing the reaction products were recorded on Bruker WH-300 spectrometer. All ^1H chemical shifts are reported in parts per million downfield relative to tetramethylsilane (TMS) as internal standard. In the assignments given below, Py refers to the pyrrole ring. All ^{13}C chemical shifts are relative to CD_3OD (δ 44.0 ppm). For determination of hydrogen substitution on C atoms, APT (attached proton test) ^{13}C NMR experiments on fully decoupled spectra were performed. The (+) and (–) signs refer to the signals above (quarternary·C and methylene-CH_2) and below (methine-CH and methyl-CH_3) the base line, respectively. High resolution mass spectra were determined using the electron ionization technique on Associated Electrical Industries (AEI) MS-9 and MS-50 focusing mass spectrometers. Optical rotation measurements were carried out on a Perkin·Elmer 241 spectropolarimeter. Kieselgel 60 (230–400 mesh) obtained from E. Merck was used for flash chromatography.

***trans*-(1*R*,2*R*)- and *trans*-(1*S*,2*S*)-1,2-Cyclopropanedicarboxylic acids (1a, 1b)** were prepared according to a published procedure[17] of ring·closing double alkylation of the succinate dianion with CH_2Br_2; the control of absolute stereochemistry of the cyclopropane ring required the use of individual isomers of menthol in the esterification of succinic acid. The individual enantiomers of bis(menthol)-1,2-cyclopropanediesters were purified by silica gel flash chromatography and subjected to hydrolysis to afford the two enantiomers of cyclopropane diacid. The final products were purified and characterized for optical purity: ^1H NMR (methanol·d_4) δ 1.37 (dd, 2 H, J = 7.2 and 7.5 Hz, C_3-H), 2.02 (dd, 2 H, $C_{1,2}$-H), 5.12 (br s, exch, 2 H, COOH); ^{13}C NMR (methanol-d_4) δ 15.65 (+, C_3), 22.93 (–, $C_{1,2}$), 175.21 (+, CO), total three signals. Specific rotations: **1a** $^{(1R,2R)}[\alpha]_D$ = – 224° (EtOH, c 1.01); **1b** $^{(1S,2S)}[\alpha]_D$ = + 209° (EtOH, c 1.04).

***trans*-(1*R*,2*R*)· and *trans*-(1*S*,2*S*)-*O*,*O*′·Bis(*N*-succinimidyl)-1,2-cyclopropanediesters (2a and 2b).** To illustrate a representative reaction,[18] a mixture of 1,2-cyclopropanedicarboxylic acid **1a** (130 mg, 1 mmol), diisopropylethylamine (284 mg, 2.2 mmol), and the commercially available (Fluka Inc.) O·(*N*-succinimidyl)-*N*,*N*,*N*′,*N*′-tetramethyluronium tetrafluoroborate (662 mg, 2.2 mmol) in 10 mL of anhydrous DMF was stirred at 30 °C for 15 h. The mixture was evaporated to dryness and extracted with CH_2Cl_2. The organic extracts were washed with water, dried (Na_2SO_4), and evaporated to afford a solid which was purified by recrystallization (MeOH) to afford 216 mg of the product **2a** (67% yield): mp 188–190 °C; ^1H NMR ($CDCl_3$) δ 1.85 (dd, 2 H, J = 7.1 and 7.5 Hz, C_3-H), 2.66 (dt, 2 H, J = 7.1 and 8.0 Hz, $C_{1,2}$-H), 2.86 (s, 8 H, $C_{3',4'}$·H); ^{13}C NMR ($CDCl_3$) δ 17.80 (+), 20.30 (–), 25.56 (+), 166.50 (+), 168.52 (+), total five signals; FAB-MS m/z 325 (M^+, 4.5%). Anal. Calcd for $C_{13}H_{12}N_2O_8$ 47.96% C, 3.72% H, 8.60% N. Found 48.49% C, 3.58% H, 8.57% N. Compound **2b** was similarly prepared from **1b**. Specific rotations: **2a** $^{(1R,2R)}[\alpha]_D$ = – 219° ($CHCl_3$, c 1.04); **2b** $^{(1S,2S)}[\alpha]_D$ = + 209° ($CHCl_3$, c 1.04).

3-(1-Methyl·4-nitropyrrole-2-carboxamido)(*N*,*N*-dimethyl)propanamine (3) was prepared from *N*-methyl·2-(trichloroacetyl)-4·nitropyrrole according to the general methods[16] reported earlier: ^1H NMR ($CDCl_3$) δ 1.72 (p, 2 H, J = 6 Hz, CH_2), 2.31 (s, 6 H, 2 × N-CH_3), 2.49 (t, 2 H, J = 6 Hz, Me_2N·CH_2), 3.47 (q, 2 H, J = 6 Hz, CONH-CH_2), 4.00 (s, 3 H, Py·NCH_3), 6.91 (d, 1 H, J = 2 Hz, Py·CH), 7.51 (d, 1 H, J = 2 Hz, Py·CH); ^{13}C NMR (CD_3OD) δ 28.12 (+), 37.92 (–), 38.69 (+), 45.41 (–), 58.22 (+), 108.44 (–), 127.83 (+), 128.36 (–), 136.11 (+), 162.55 (+), total of 10 signals.

3-[1·Methyl-4-(1-methyl-4-nitropyrrole-2-carboxamido)pyrrole-2-carboxamido](*N*,*N*-dimethyl)propanamine (4) was also prepared from **3** and *N*-methyl-2-(chloroacetyl)-4-nitropyrrole according to the general methods[16] of peptide coupling reported for the preparation of netropsin and distamycin analogs: ^1H NMR (DMSO-d_6) δ 1.61 (p, 2 H, J = 6 Hz, CH_2), 2.14 (s, 6 H, 2 × N·CH_3), 2.24 (t, 2 H, J = 6 Hz, Me_2N-CH_2), 3.19 (q, 2 H, J = 6 Hz, CONH-CH_2), 3.80 and 3.96 (2 s, 3 H each, 2 × Py·NCH_3), 6.81 and 7.20 and 7.58 and 8.18 (4 d, 1 H each, J = 2 Hz, 4 × Py·CH), 8.11 (exch t, 1 H, J = 6 Hz, CH_2NH), 10.22 (exch s, 1 H, CONH); ^{13}C NMR (methanol-d_4) δ 28.03 (+), 36.76 (–), 37.99 (–), 38.41 (+), 45.19 (–), 58.19 (+), 105.68 (–), 108.69 (–), 120.42 (–), 122.85 (+), 124.73 (+), 127.78 (+), 128.64 (–), 136.16 (+), 159.60 (+), 164.17 (+), total of 16 signals; FAB·MS m/z 377 (M^+, 73%).

(18) Knorr, R.; Trzeciak, A.; Bannwarth, W.; Gillessen, D. *Tetrahedron Lett.* **1989**, *30*, 1927–1930.

***trans*-(1*R*,2*R*)- and *trans*-(1*S*,2*S*)-*N*,*N*′-Bis{5-[[[5-[[(3-(dimethylamino)propyl)amino]carbonyl]-1-methyl-1*H*-pyrrol-3-yl]amino]carbonyl]-1·methyl-1*H*-pyrrol-3-yl}-1,2-cyclopropanedicarboxamide Dihydrochloride [(1*R*,2*R*)-BNC and (1*S*,2*S*)-BNC].** The preceding compound **4** (452 mg, 1.2 mmol) was hydrogenated in 40 mL of solvent mixture of DMF–MeOH (1:4 v/v) in the presence of 10% Pd-C (200 mg) at atmospheric pressure for 6 h. The mixture was filtered through Celite, and the filtrate was evaporated to remove methanol. The solution obtained was diluted further with 10 mL of DMF and cooled to 0 °C. A solution of bis(*N*-succinimidyl)-1,2-cyclopropanediester (**2a**) (163 mg, 0.5 mmol) in 5 mL of DMF was then added dropwise under Ar to the preceding solution. At the completion of addition, the reaction mixture was allowed to warm to 25 °C and stirred further for 14 h. Evaporation of the solvent afforded an oily residue which was dissolved in a mixture of 10 mL of EtOH and 2 mL of aqueous HCl (1 N). Evaporation of the solvent gave the dihydrochloride salt which was crystallized from EtOH–Et_2O and lyophilized to afford 307 mg (71% yield) of the product (**1*R*,2*R*)-BNC**: mp 206–209 °C; ^1H NMR (DMSO-d_6) δ 1.23 (t, 2 H, J = 7 Hz, cyclopropyl CH_2), 1.87 (p, 4 H, J = 7.5 Hz, 2 × CH_2), 2.20 (t, 2 H, J = 7 Hz, cyclopropyl CH), 2.74 (2 s, 6 H each, 4 × N-CH_3), 3.02 (t, 4 H, J = 7.5 Hz, 2 × Me_2N-CH_2), 3.22 (q, 4 H, J = 6 Hz, 2 × CONH·CH_2), 3.80 (2 s, 6 H each, 4 × Py-NCH_3), 6.87 (d, 2 H, J = 1.5 Hz, Py-CH), 6.91 (d, 2 H, J = 1.5 Hz, Py-CH), 7.17 (d, 2 H, J = 1.5 Hz, Py-CH), 7.18 (d, 2 H, J = 1.5 Hz, Py-CH), 8.17 (exch t, 2 H, J = 6 Hz, 2 × CH_2-NH), 9.88 (exch s, 2 H, 2 × CONH), 10.37 (exch s, 2 H, CONH); ^1H NMR (methanol-d_4; 500 MHz) δ 1.39 (t, 2 H, J = 7 Hz, cyclopropyl CH_2), 1.98 (p, 4 H, J = 7.5 Hz, 2 × CH_2), 2.22 (t, 2 H, J = 7 Hz, cyclopropyl CH), 2.89 (s, 12 H, 4 × N-CH_3), 3.15 (t, 4 H, J = 7.5 Hz, 2 × Me_2N-CH_2), 3.40 (t, 4 H, J = 7.5 Hz, 2 × CONH-CH_2), 3.88 (s, 12 H, 4 × Py-NCH_3), 6.81 (d, 2 H, J = 1.5 Hz, Py-CH), 6.89 (d, 2 H, J = 1.5 Hz, Py-CH), 7.14 (d, 2 H, J = 1.5 Hz, Py-CH), 7.16 (d, 2 H, J = 1.5 Hz, Py·CH); ^{13}C NMR (methanol·d_4) δ 14.04 (+), 24.13 (–), 26.54 (+), 36.68 (–), 36.79 (–), 36.88 (+), 43.57 (–), 56.71 (+), 105.81 (–), 106.68 (–), 120.61 (–), 120.91 (–), 123.37 (+), 123.39 (+), 123.93 (+), 124.62 (+), 161.37 (+), 164.91 (+), 170.48 (+), total of 19 signals. Compound **(1*S*,2*S*)·BNC** was prepared from **2b** using the same procedure. Specific rotations: $^{(-)\cdot(1R,2R)}[\alpha]_D$ = – 108° (MeOH, c 0.72); $^{(+)\cdot(1S,2S)}[\alpha]_D$ = + 101° (MeOH, c 0.72).

DNA Synthesis. The self-complementary dodecamer d(CGAAA·ATTTTCG) was synthesized and purified according to standard protocol of automated solid support DNA synthesis on a ABI DNA synthesizer. The purity of the DNA sample was checked by reverse-phase HPLC and ^1H NMR for any residual organic impurities.

High-Field NMR Measurements. NMR samples were prepared by dissolving the dodecamer oligonucleotide (18 mg) in 800 μL of 10 mM sodium phosphate buffer (pH 6.68) containing 10 mM sodium chloride. The solution was divided into two equal portions. Each sample was lyophilized to dryness and further elaborated for NMR experiments in an identical manner. For experiments carried out in D_2O, the solid was lyophilized twice from 99.9% D_2O and finally redissolved in 0.65 mL of 99.96% D_2O. For experiments in H_2O, the solid was redissolved in 9:1 H_2O/D_2O mixture to a final volume of 0.65 mL.

The stock solutions of (1*R*,2*R*)- and (1*S*,2*S*)·BNC were prepared by dissolving 10 mg of each ligand in 10 mL of 99.96% D_2O and stored at –20 °C in dark. The concentrations of the stock solutions were adjusted to an identical value of 1.14 mM, by measuring UV absorbance at 300 nm (ϵ = 35 800 M^{-1} cm^{-1}). Titrations were performed by adding 0.2 mol equiv of ligand solutions into the NMR samples of the DNA, and NMR spectra were recorded at each stage over the temperature range of 5–50 °C (at 5 °C intervals). The mixtures containing 1:1 molar ratios of the ligand and DNA are termed DNA–ligand complexes which were characterized extensively using two dimensional NMR experiments.

The proton one· and two-dimensional spectra were acquired on a Varian Unity 500-MHz spectrometer. The one·dimensional ^1H NMR spectra of the dodecamer and that of the dodecamer–ligand complex were acquired during a titration experiment involving stepwise additions of a freshly prepared stock solution of the ligand to the NMR sample of the oligonucleotide. The 1D spectra were acquired at 294 K using a sweep width of 5000 Hz, 128 scans, and 32 k data points. A presaturation pulse during the recycle delay of 3 s was used to suppress the residual HOD resonance. The data were processed with a Gaussian apodization function (interactively adjusted to ensure decay of FID to zero) to provide resolution enhancement.

Spectra showing the exchangeable imino protons of the free DNA and the DNA–ligand complexes were obtained by using the Sklenar–Bax water suppression scheme[19] on the sample dissolved in 9:1 H_2O–D_2O. These spectra were collected with a sweep width of 10 000 Hz, a 90°

pulse of 8.5 μs, and 32 k data points. The delay time between the 90° pulses was optimized to 7.4 ms with a spin-lock pulse of duration 2 ms, in order to maximize the HOD suppression and selective observation of the imino signals. The data were Fourier transformed with 3 Hz line broadening.

Two-dimensional NOESY experiments on the DNA and the DNA–ligand complexes were performed on nonspinning samples in the phase-sensitive mode according to the hypercomplex method[20] by use of standard NOESY pulse sequence provided in the Varian vnmr software. For each sample a series of such experiments were done for mixing intervals of 80, 150, 200, 250, and 400 ms. The interproton distances r_{ij} were estimated from the magnitude of cross peaks in NOESY spectra acquired with recycle time of 5 s and mixing time of 200 ms, using the isolated spin pair approximation (ISPA) relationship: $r_{ij} = (v_{ref}/v_{ij})^{1/6} r_{ref}$. The cross peak volume integrals v_{ij} for the assessment of relative intensities were determined for individual cross peaks by evaluating the average volumes (peak height × area) for a series of equally sized rectangles circumscribing each peak. The cytosine H5·H6 interproton vector was taken to be a reference distance of 2.46 Å,[23d] and the distance estimates were accurate to within a few percent for other fixed distances in the molecule, e.g., thymidine H6-Me, intraresidue H2′·H2″ etc. The longest mixing time NOESY spectra were obtained for the purposes of complete assignment of the nonexchangeable proton signals. Data were acquired with the carrier frequency at the center of the spectrum and quadrature detection for a sweep width of 4500 Hz (adjusted to cover the entire range of the signals due to the nonexchangeable protons) in both the t_1 and t_2 dimensions. Data sets consisted of 512 FIDs (t_1) and 2048 data points in t_2. A relaxation delay interval of 2.0 s was set for each pulse sequence. The spectra were zero-filled to 2048 points in t_1 prior to Fourier transformation thus relating to equal digital resolution of ~4 Hz in both dimensions. In order to avoid truncation of the free induction decays, a skewed sinebell apodization function was set interactively to ensure that the interferrograms decayed to zero in both t_1 and t_2 dimensions. The baseline corrections were performed as previously reported.[21]

Thermal Denaturation (T_m) Measurements. Commerically available (*Sigma*) polymer DNA sequences poly(dA), poly(dT), and poly(dA)·poly(dT) were used for these measurements. The thermal denaturation temperature of DNA sequences and their complexes with the ligands were determined in 20 mM phosphate buffer, pH 6.6, containing 100 mM NaCl, 10 μM EDTA, and 28 μM DNA phosphate (concentration is expressed in terms of phosphate due to undetermined length of strands in the polymer duplexes), with added amounts of ligand solutions according to the desired ratios of ligand to base pair. Melting curves were recorded on a Varian CARY 210 UV/vis spectrophotometer equipped with a jacketed cuvette holder, which was heated by a solution of ethylene glycol from a LKB·BROMMA 2019 multiheat thermostatic circulator. The cell temperature was recorded by a thermocouple inserted into the cell block. At the end of each experiment, the data were saved to disk and analyzed on a Macintosh personal computer using Cricketgraph software. Selction of the midpoint (T_m) value of the temperature/absorbance curve was made from the first order differential plots as shown in the supplementary material on ΔT_m curves.

Computations on Structure Refinements and Restrained Molecular Modeling. The enantiomer molecules (1*R*,2*R*)- and (1*S*,2*S*)-BNC with fixed absolute configuration at the cyclopropane ring were constructed using the program Macromodel V3.5X.[22a] The structures were energy minimized using the modified MM2 parameters,[22a] and the coordinates were further optimized with the program MOPAC ESP.[22b] The results on the final geometry and electrostatic potential charges were then used to build the input file for subsequent incorporation in AMBER 4.0.[22c]

The DNA duplex d(CGAAAATTTTCG)$_2$ was constructed in AMBER 4.0 using Arnott's B·DNA coordinates.[22d] Energy minimization was first done in vacuo with a distance dependent dielectric constant until the rms deviation was less than 0.1 kcal·mol^{-1}·Å. Steepest descent was used for the first 100 cycles and for 10 cycles after each update of the nonbonded pair list; otherwise the conjugate gradient approach was in effect. In order to attenuate the charges on the phosphate groups, 22 sodium counterions were then added to the model at a distance of 3.0 Å from the phosphorus atoms within the phosphate O–P–O planes. The now charge-balanced system was reminimized in vacuo using the same conditions as above. The post-solvation model, obtained by immersion in a box of TIP3P water molecules with a minimum solvent shell thickness of 10 Å from DNA and counterions, was next subjected to a "belly" minimization and molecular dynamics at constant volume followed by the same at constant pressure. In the first solvated minimization a belly is placed on the DNA and counterions so that they are "frozen" and only the surrounding water molecules are allowed to move. This was done for 200 cycles with a 9.0 Å cutoff (all solvated simulations use this value) with a switch from steepest descent to conjugate gradient after 100 cycles. The next step served to randomize the water molecules around the DNA and counterions. While the solute remained fixed, the water molecules were allowed to move for the next 1000 steps (0.001 ps step size) at a temperature of 10 K up to 300 K under constant volume conditions. At the end of this run, the velocities were discarded, and the simulation was allowed to proceed without any belly atoms. The time step was increased to 0.002 per step, and the temperature was raised from 10 K to 300 K in steps of 5 K over the first 10 ps. This was followed by 40 ps of productive dynamics under the same conditions, while the temperature was kept regulated at 300 ± 5 K. The final complex at the end of runs was reminimized as above with the belly groups removed until the rms deviation was <0.1 kcal·mol^{-1}·Å.

Minimizations on the diasteromeric complexes (1*R*,2*R*)· and (1*S*,2*S*)-BNC:DNA were performed using MidasPlus[22e] and the experimentally obtained intermolecular DNA·ligand NOE distance constraints for docking. Similar energy values were chosen as those already existing in the all atom force field[22e] and the angles were defined according to the geometry obtained from MOPAC ESP.[22b] The rest of the procedures for minimizations were performed as recorded above for the DNA duplex itself. The constraints derived from the experimental NMR data were introduced gradually beginning at the 5 ps mark (by increasing the scaling factor from 0–2 at the 10 ps mark) and maintained at this level until the end of simulations. The final structures for the complexes were reminimized as above with the belly groups removed until the rms deviations were <0.1 kcal·mol^{-1}·Å.

Results

NMR Analysis of Free Duplex d(CGAAAATTTTCG)$_2$. In order to characterize and compare the noncovalent interactions of optically pure (1*R*,2*R*)- and (1*S*,2*S*)-BNC with d(CGAAAATTTTCG)$_2$ on the basis of NOE effects, the corresponding ^{1}H NMR spectrum of the ligand-free dodecanucleotide had first to be assigned completely. Standard methods of delineating individual spin systems of deoxyribose units in correlation spectra and sequential intra- and interresidue NOE connectivities in NOESY spectra of right-handed B-type DNA structures were used for this purpose.[23] Thus, a complete set of the nonexchangeable glycosidic and aromatic base proton assignments was obtained from phase-sensitive NOESY spectra (Figure S1, supplementary material) acquired on a buffered D_2O solution (pH 6.68; 30 °C) of d(CGAAAATTTTCG)$_2$ by first identifying two independent magnetization transfer pathways involving (i) the glycosidic H1′ and (ii) the H2′/H2″ protons to the purine/pyrimidine base protons and secondly confirmed by cross-checks in other regions of the NOESY plots. A part of this strategy is illustrated in Figure 3, with a continuous connectivity pathway for the full length of the DNA sequence from C_1 to G_{12}, and the proton chemical shifts are tabulated in Table 1. The centrally located unique 5′-AT site served as a useful starting point to identify the A_6H8 resonance at 7.97 ppm via a strong NOE to the T_7CH3 at 1.17 ppm (Figure S2, supplementary

(19) Sklénar, V.; Bax, A. *J. Magn. Reson.* **1987**, *74*, 469–479.
(20) (a) States, D. J.; Haberkorn, R. A.; Ruben, D. J. *J. Magn. Reson.* **1982**, *48*, 286–292. (b) Bodenhausen, G.; Kogler, H.; Ernst, R. R. *J. Magn. Reson.* **1984**, *58*, 370–388.
(21) Otting, G.; Widmer, H.; Wagner, G.; Wüthrich, K. *J. Magn. Reson.* **1986**, *66*, 187.
(22) (a) Still, W. C. *Macromodel V3.5X Interactive Molecular Modeling System*, Columbia University: New York, 1992. (b) Besler, B. H.; Merz, K. M.; Kollman, P. A. *J. Comput. Chem.* **1990**, *11*, 431–439. (c) Pearlman, D. A.; Case, D. A.; Caldwell, J. C.; Seibel, G. L; Singh, U. C.; Weiner, P. K.; Kollman, P. A. *AMBER 4.0*, University of California, San Francisco, 1991. (d) Ferrin, T. E.; Huang, C. C.; Jarvis, L. E.; Langridge, R. *J. Mol. Graphics* **1988**, *6*, 13–27. (e) Weiner, S. J.; Kollman, P. A.; Case, D.; Singh, U. C.; Ghio, C.; Alagona, G.; Prafeta, S.; Weiner, P. K. *J. Am. Chem. Soc.* **1984**, *106*, 765–784.
(23) (a) Feigon, J.; Leupin, W.; Denny, W. A.; Kearns, D. R. *Biochemistry* **1983**, *22*, 5943–5951. (b) Hare, D. R.; Wemmer, D. E.; Chou, S.·H.; Drobny, G.; Reid, B. *J. Mol. Biol.* **1983**, *171*, 319–336. (c) Scheek, R. M.; Boelens, R.; Russo, N.; van Boom, J. H.; Kaptein, R. *Biochemistry* **1984**, *23*, 1371–1376. For general reviews on these aspects, see: (d) Gronenborn, A. M.; Clore, G. M. *Prog. Nucl. Magn. Reson. Spectrosc.* **1985**, *17*, 1–32. (e) Reid, B. R. *Quart. Rev. Biophys.* **1987**, *20*, 1–34. (f) Patel, D. J.; Shapiro, L.; Hare, D. *Annu. Rev. Biophys. Biophys. Chem.* **1987**, *16*, 423–454.

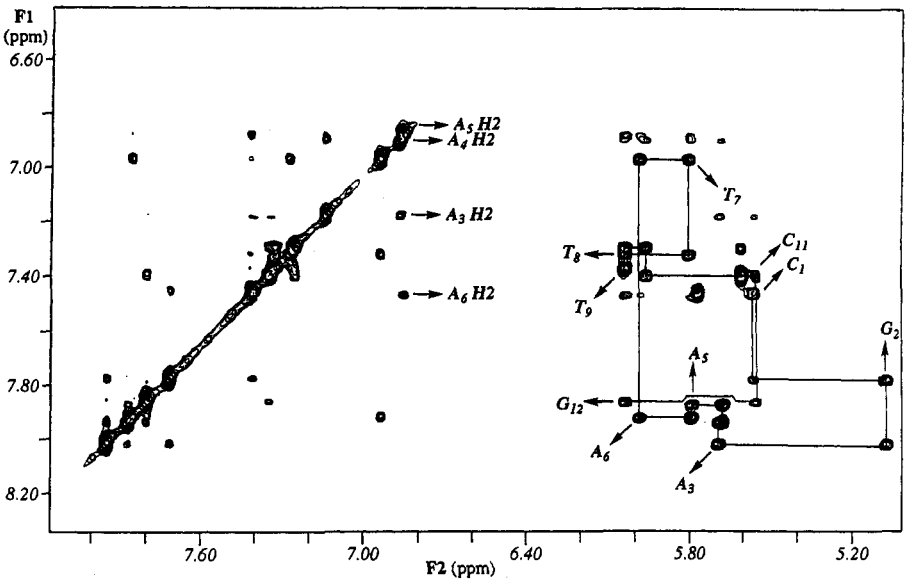

Figure 3. Expanded subsections of the contour plot of a phase-sensitive 2D-NOESY spectrum at 500 MHz of a D_2O buffered solution of duplex d(CGAAAATTTTCG)$_2$ at 298 K and pH 6.68 (uncorrected, 20 mM phosphate), showing the cross peaks between (a) the purine/pyrimidine base protons and glycosidic H1′ protons. Continuous lines illustrate the sequential NOE connectivities from C^1 through G^{12}.

Table 1. Chemical Shift Assignments (in ppm) of Protons in d(CGAAAATTTTCG)$_2$, Determined from Two-Dimensional NOESY Spectra Recorded at 313 K in 20 mM Phosphate Buffer in D_2O, pD = 6.68 (Uncorrected).

	H8/H6	H5/H2/Me	H1′	H2″	H2′	H3′	imino[a]
C1	7.57	5.89	5.71	2.21	1.64	4.58	
G2	7.83		5.18	2.57	2.48	4.87	12.97
A3	8.07	7.30	5.77	2.75	2.59	4.98	
A4	7.99	7.04	5.76	2.78	2.51	4.97	
A5	7.93	6.99	5.86	2.84	2.75	4.97	
A6	7.97	7.55	6.08	2.87	2.44	4.95	
T7	7.03	1.17	5.88	2.56	1.96	4.81	13.88
T8	7.38	1.47	6.12	2.17	1.79	4.88	14.14
T9	7.42	1.59	6.11	2.60	2.14	4.85	14.02
T10	7.37	1.64	6.04	2.45	2.08	4.87	13.86
C11	7.49	5.73	5.76	2.34	2.00	4.80	
G12	7.90		6.12	2.59	2.42	4.64	13.18

[a] At 278 K, in 90% H_2O–D_2O, using 11 echo pulse for solvent suppression.

material). An interesting feature observed from the chemical shift assignments pertains to an unusual resonance of G_2H1′ at 5.18 ppm which is shifted upfield in the range of 0.53–0.96 ppm from the rest of the residues, evidently due to the ring current effects from the immediately following adenine-tract in this sequence.[24]

A number of additional cross peaks relating to adenine H2 protons were also observed in the base/H1′ regions of the NOESY spectra for this sequence containing a contiguous 5′-AAAA-3′ stretch and a central 5′-AT step. These strong interactions were identified as sequential and interstrand connectivities with the proximally located sugar H1′ protons along the adenine-tract presumably due to highly propeller twisted AT base pairs and a narrow minor groove width of the AT tract.[25] The assignment of the adenine H2 protons is further confirmed via sequential adenine H2-H2 contacts (Figure 3) along with their 2D-NOE cross peaks with the flanking exchangeable imino protons that are observed in the NOESY spectra (Figure S3, supplementary material) acquired in buffered (9:1 H_2O/D_2O solutions (pH 6.68; 5 °C).

Although certain features of an adenine-tract containing "bent" DNA structure[26] are evident as noted above, the overall right-handed B-type conformation for d(CGAAAATTTTCG)$_2$ was confirmed as supported by an inspection of the relative intensities of the characteristic cross peaks in the NOESY spectra acquired with different mixing time intervals. For example, the intraresidue base/H2′ and interresidue base/H2″ cross peaks were present even at shorter mixing intervals of 50–80 ms, while those for intraresidue base/H2″ and interresidue base/H2′ protons build up at longer mixing times. An overall order of relative intensities[27] for the cross peaks between base protons and H2′ $\gg$ H1′ $\geq$ H3′ at rather short mixing intervals (100–180 ms) where the overestimations due to spin diffusion are minimized further supports the derived B-DNA conformation.

General Characteristics of Dodecanucleotide Complexes with (1*R*,2*R*)- and (1*S*,2*S*)-BNC. The general characterization of the noncovalent binding of ligands (1*R*,2*R*)- and (1*S*,2*S*)-BNC to d(CGAAAATTTTCG)$_2$ was achieved by NMR titration experiments performed by adding small aliquots of D_2O solutions of the ligand to a sample of dodecanucleotide to final stoichiometries corresponding to 1:1 molar ratios of ligand to DNA and monitoring the changes in the nonexchangeable proton resonances. Under the conditions of these NMR experiments, a general increase in the line widths of the resonances over much of the spectra, in particular of the well-resolved ligand aromatic and DNA base protons, as a result of an increased correlation time provide qualitative evidence for binding of the ligands to the dodecamer, as determined from the respective 500-MHz ^{1}H NMR spectra of the nonexchangeable protons of d(CGAAAATTTTCG)$_2$ and its 1:1 complexes with (1*R*,2*R*)-BNC and (1*S*,2*S*)-BNC (data not shown). In addition to the qualitative line broadening arguments and other evidence for binding, which is described below, the twofold dyad symmetry of the self-complementary duplex sequence appears to be retained in each complex as evident from the four well separated T-CH_3 signals in the spectra of the free duplex and the complexed forms.

It is known from previous structural studies on ligand–DNA complexes of netropsin and distamycin that these oligopyrrolecarboxamides span 4–5 AT base pairs.[3,5,6] Several monodentate binding modes are therefore possible in the present analysis of complexes of (1*R*,2*R*)- and (1*S*,2*S*)-BNC, each of which contains two symmetrically disposed netropsin subunits, with d(CG-

(24) Katahira, M.; Sugeta, H.; Kyogoku, Y.; Fujisawa, R.; Tomita, K. *Nucleic Acids Res.* **1988**, *16*, 8619–8632.

(25) (a) Sarma, M. H.; Gupta, G.; Sarma, R. H. *Biochemistry* **1988**, *27*, 3423–3432. (b) Gupta, G.; Umemoto, K.; Sarma, M. H.; Sarma, R. H. *Int. J. Quant. Chem.: Quant. Biol. Symp.* **1989**, *16*, 17–33. (c) Celda, B.; Widmer, H.; Leupin, W.; Chazin, W. J.; Denny, W. A.; Wüthrich, K. *Biochemistry* **1989**, *28*, 1462.

(26) Hagerman, P. J. *Annu. Rev. Biochem.* **1990**, *59*, 755–781.

(27) *NMR of Proteins and Nucleic Acids*; Wüthrich, K., Ed; Wiley: New York, 1986; pp 203–255.

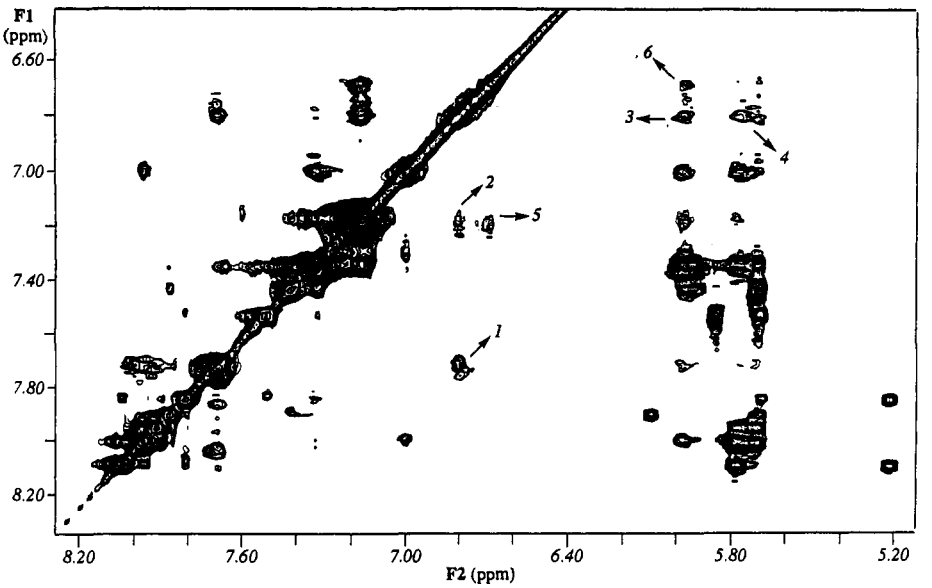

Figure 4. The expanded spectral regions of a 200 ms phase-sensitive 2D-NOESY spectrum of the 1:1 complex formed between the (1*R*,2*R*)-BNC ligand and d(CGAAAATTTTCG)$_2$ at 313 K, showing cross peaks corresponding to intra- and internucleotide connectivities as in Figure 3a along with intermolecular NOE interactions between the ligand and DNA protons. A complete list of the latter is provided in Table 3.

AAAATTTTCG)$_2$ which has five overlapping potential binding sites that are 4 AT base pair long. Thus, initial monodentate binding of the individual netropsin halves of the extended ligands in a fixed orientation could occur at 5′-AAAA, 5′-AAAT, 5′-AATT, 5′-ATTT, or 5′-TTTT, and each of them would be expected to lift the molecular twofold symmetry of the double stranded DNA sequence as a result of nonequivalence of the two strands. Such a scenario should then result in a doubling of DNA protons resonances as normally observed for binding of asymmetric minor groove binding agents.[5,13,28] We do not observe this experimentally for either of the complexes, over the temperature range of 5–50 °C, even at intermediate stages of the titration experiments indicating that both the netropsin subunits bind simultaneously in each case, conceivably at the two symmetry related 5′-AAAA sites. The bidentate cooperative binding[10b,c] appears relatively stronger than monocomplexation of one-half of the molecules due to the presence of two equivalent sites and/or is dictated by the inherent affinity of the individual neotropsin half toward an all-A (or the complementary all-T) stretch namely 5′-AAAA.

The ^{1}H NMR spectra acquired in 9:1 H_2O/D_2O with signals corresponding to the imino protons in the base pairs of d(CGAAAATTTTCG)$_2$ itself and its complexes with (1*R*,2*R*)- and (1*S*,2*S*)-BNC also showed six resonances without any apparent doubling in the complexed forms. The lack of doubled signals, which could reflect asymmetric binding modes, indicates tight bidentate binding of the two symmetrical ligands in their fully extended form at the centrally located 8 base-pairs long AT-rich core with the cyclopropane linker template at the central 5′-AT step so that the twofold symmetry of the DNA duplex is retained in each case.

NMR Analysis of (1*R*,2*R*)-BNC:d(CGAAAATTTTCG)$_2$ Complex. Resonance assignments in the (1*R*,2*R*)-BNC:d(CGAAAATTTTCG)$_2$ complex were obtained, using the same principles as mentioned above for the assignments of the ligand-free DNA, by employing the standard methods of delineating sequential connectivities in the "fingerprint" regions of 2D-NOESY plots.[23] Each aromatic base proton (purine H8, pyrimidine H6) was assigned through its NOE interaction with the H1′ of its own sugar and the H1′ of its 5′-neighbor (Figure 4) and further confirmed by similar connectivities with the intra- and internucleotide H2 and H2″ protons. Significantly, the NOE cross peaks associated with the sequential and interstrand connectivities between the adenine H2 and sugar H1′ protons suffered from an intensity loss in the presence of the bound ligand. Although the loss of NOE cross peak intensities could arise from line broadening, it can also be attributed to a tight binding of the ligand at the AT-tract, which causes an opening of the minor groove to release the high propeller twist in the AT base pairs, observed in the case of the free DNA itself.

The pyrrole H3/H9 protons lining the concave edge and the pyrrole H5/H11 protons lining the convex edge of the ligand were assigned through their NOE interactions with the adjacently positioned amide N1H/N3H and the pyrrole methyl N2CH3/N4CH3 protons, respectively, from the 2D-NOESY experiments in 9:1 H_2O/D_2O and D_2O buffer solutions as described in earlier NMR investigations on drug–DNA complexes of netropsin and distamycin.[5,28b] The scalar coupled protons in the aliphatic regions, belonging to the cyclopropane and dimethylaminopropyl groups, were assigned from the homonuclear correlation (COSY) experiments. The ligand proton assignments are summarized in Table 2 for both (1*R*,2*R*)- or (1*S*,2*S*)-BNC in complexes with d(CGAAAATTTTCG)$_2$.

The most significant points of close contact between the ligand protons and the minor groove marker protons (e.g., adenine-H2s at the groove floor and the sugar H1′ protons) are often identified by the associated intermolecular NOE interactions.[5d-f,28] The partial NOESY spectrum of the (1*R*,2*R*)-BNC:d(CGAAAATTTTCG)$_2$, shown in Figure 4, reveals numerous intermolecular NOE interactions that provide strong evidence for minor groove binding and permit us to define the binding location and the relative orientation of (1*R*,2*R*)-BNC on the DNA. Some of these, for example, are strong NOE cross peaks as observed between the pyrrole H3 and H9 protons (both on the concave face) and the H2 protons of A_6 and A_4, respectively. In addition, a preference for association with the strand containing T-residues is indicated by NOE interactions between the same pyrrole H3/H9 protons and the sugar H1′ protons of T_7, T_8, and T_9, respectively. These ligand–DNA contacts [summarized in Table 3A and Figure 5a], along with the requirement of a symmetric arrangement, form the basis of illustrating a nearly perfect isohelical docking of the entire ligand molecule with a bidentate association of the two netropsin arms in an end-to-end fashion in the minor groove of 5′-(A)$_4$(T)$_4$ segment, and with the cyclo-

(28) (a) Leupin, W.; Chazin, W. J.; Hyberts, S.; Denny, W. A.; Wüthrich, K. *Biochemistry* **1986**, *25*, 5902–5910. (b) Singh, M. P.; Kumar, S.; Joseph, T.; Pon, R. T.; Lown, J. W. *Biochemistry* **1992**, *31*, 6453–6461. (c) Singh, M. P.; Joseph, T.; Kumar, S.; Bathini, Y.; Lown, J. W. *Chem. Res. Toxicol.* **1992**, *5*, 597–607, and references therein.

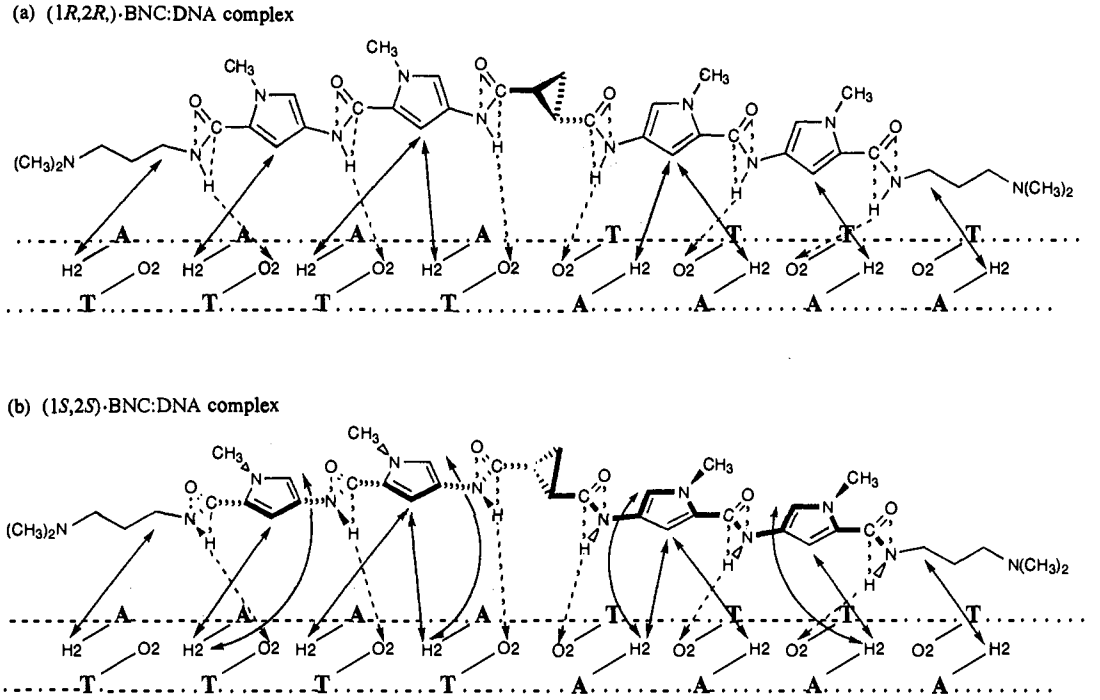

Figure 5. Schematic representations of the inferred model orientations from intermolecular NOE data, indicating isohelical and strand-selective binding of the BNC ligands to 5′-AAAATTTT segments on duplex DNA, illustrated by experimentally observed intermolecular NOE contacts (solid double headed arrows), and possible hydrogen bonding (broken arrows) between d-(CGAAAATTTTCG)$_2$ and (a) (1*R*,2*R*)-BNC with a right-handed twist at the cyclopropane linker and (b) (1*S*,2*S*)-BNC with a left-handed cyclopropane and the netropsin arms predisposed away from 5′-TTTT sites; in order to afford the depicted hydrogen-bonding, the planar amide groups must twist (along ψ_1, ψ_3, and ψ_5) along with a counterclockwise twist of the pyrrole rings (ψ_2 and ψ_4) which is detected by intermolecular NOE interactions from the protons on both the concave and convex edges of the ligand. For definition of angles, see Figure 2c.

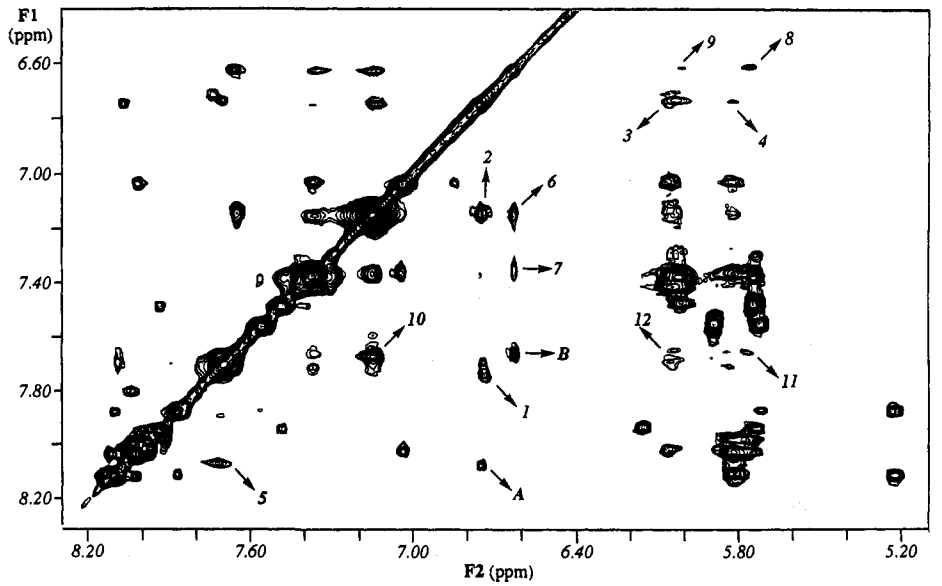

Figure 6. The expanded regions of a 200 ms phase-sensitive 2D-NOESY spectrum of the 1:1 complex formed between ligand (1*S*,2*S*)-BNC and d(CGAAAATTTTCG)$_2$ at 313 K. The description is analogous to that for Figure 4.

propane linker at the central 5′-AT step and its methylene group projecting away from it.

NMR Analysis of DNA Complex with Enantiomeric (1*S*,2*S*)-BNC. Nonexchangeable and exchangeable proton assignments were made for the diasteromeric (1*S*,2*S*)-BNC:d(CGAAAATTTTCG)$_2$ complex using similar arguments of tracing sequential connectivities as above for the free DNA and the complex with (1*R*,2*R*)-BNC. An expansion of the NOESY spectrum (Figure 6) of the (1*S*,2*S*)-BNC:d(CGAAAATTTTCG)$_2$ complex shows NOE interactions in the aromatic base to sugar H1′ regions. The NOE cross peaks corresponding to C_1H6-H5, C_9H6-H5, and A_6H8-T_7Me are good starting markers for the assignment procedure, as found in the case of free DNA, which was extended to obtain the complexation-induced chemical shift differences (summarized in Table T1, supplementary material). Several similarities were observed between the two complexes in terms of the NOE interactions between DNA protons and the apparent lack of binding-induced asymmetry in the complexed forms which indicates a similar bidentate mode of binding of (1*S*,2*S*)-BNC as observed for (1*R*,2*R*)-BNC. A comparison of the chemical shift values for the DNA and the ligand protons reveals subtle differences in the two diastereomeric complexes which differ only in terms of the chirality at the central cyclopropane template.

A further comparative inspection of the intermolecular NOE contacts observed for the (1*S*,2*S*)-BNC complex with those in

Table 2. Chemical Shift Assignments (δ, ppm) and Complexation-Induced Chemical Shift Differences ($\Delta\delta$, ppm) for the (1*R*,2*R*)- and (1*S*,2*S*)-BNC Ligand Protons upon Binding to d(CGAAAATTTTCG)$_2$, Determined from Two-Dimensional NOESY Spectra at 313 K in 20 mM Phosphate Buffered D_2O, pD = 6.68 (Uncorrected). [See Figure 2 for the Numbering System]

		(1R,2R)-BNC		(1S,2S)-BNC	
	free ligand	δ	$\Delta\delta$	δ	$\Delta\delta$
		Toward DNA Minor Groove			
C17	2.74	2.92	−0.18	2.96	−0.22
C16	3.02	3.19	−0.17	3.21	−0.19
C15	1.87	2.01	−0.14	2.03	−0.16
C14	3.22	3.37	−0.15	3.41	−0.19
N5	8.17	8.95	−0.78	8.95	−0.78
C9	6.87	6.68	0.19	6.61	0.28
N3	9.88	10.05	−0.17	10.06	−0.18
C3	6.91	6.79	0.12	6.74	0.17
N1	10.37	10.58	−0.21	10.55	−0.18
C1′	2.20	3.30	−1.10	3.32	−1.02
C2′	2.20	3.30	−1.10	3.32	−1.02
		Away from DNA Minor Groove			
C17	2.74	2.92	−0.18	2.96	−0.22
C16	3.02	3.19	−0.17	3.21	−0.19
C15	1.87	2.01	−0.14	2.03	−0.16
C14	3.22	3.37	−0.15	3.41	−0.19
C12	3.80	3.64	0.16	3.98	−0.18
C11	7.18	7.60	−0.42	7.66	−0.48
C6	3.80	3.74	0.06	4.03	−0.20
C5	7.17	7.85	−0.68	8.07	−0.90
C3′	1.23	2.01	−0.82	2.01	−0.82
C1′	2.20	3.30	−1.10	3.32	−1.02
C2′	2.20	3.30	−1.10	3.32	−1.02

the (1*R*,2*R*)-BNC complex was important since the minor groove binding netropsin components of the two ligands are chemically identical and any differences between enantiomers would then depend solely on the disposition of DNA-binding units about the rigid cyclopropane linker. The evidence for such changes is provided by a greater number of NOE cross peaks between minor groove marker H2 protons of adenine residues and the protons on both the concave and convex edges of the pyrrole units in the case of (1*S*,2*S*)-BNC:d(CGAAAATTTTCG)$_2$ as shown in Figure 5b. Thus, strong NOE interactions [with the corresponding peaks labeled in Figure 6 and listed in Table 3B] are observed for the H2 proton of A_6 with the pyrrole H3 proton on the concave face (peak labeled 1) as well as with the pyrrole H5 proton on the convex face (peak labeled 5). A similar pattern of intermolecular NOEs is seen for the H2 proton of A_4 with the H9 proton on the concave (peak labeled 6) and the H11 proton on the convex (peak labeled 10) faces of the second outer pyrrole units of (1*S*,2*S*)-BNC. Numerous other intermolecular NOE contacts were also identified and are summarized in Table 3B.

Collectively, these intermolecular ligand–DNA interactions are consistent with the binding site location and orientation analogous to that shown above for (1*R*,2*R*)-BNC with an important difference in the relatively noncoplanar arrangement of the *N*-methylpyrrole rings, as illustrated in Figure 5b. Such a binding-induced twist of the two pyrrole rings of each of the netropsin subunits only can explain the observed NOEs between the DNA protons and the protons lining the two edges of the ligand. The dihedral angles of 20° and 33° for a skewed twist of the pyrrole rings have previously been observed in the X-ray crystal structures of the netropsin molecule[6a] and of its complex with Dickerson's dodecamer,[6b-d] respectively. Deviations from planarity, as large as a dihedral angle of 68° between adjacent pyrrole rings, have also been observed in a recent study on a distamycin analog complexed with an A_3T_3 site-containing dodecamer.[29] An experimentally detectable consequence of such a rotation of the pyrrole rings in the case of the (1*S*,2*S*)-BNC: DNA complex is that additional pathways of spin-diffusion are established which were identified by the NOE cross peaks (Figure 6) between the ligand pyrrole protons H3-H5 (peak labeled A) and H9-H11 (peak labeled B), evidently due to the DNA protons A_6H2 and A_4H2, respectively, in the roles of their common partners. The most plausible explanation for the observed twisting of the pyrrole rings is attributed to the adjustments required by the hydrogen-bonding between the ligand amide NHs and the (5′-TTTT) contiguous arrangement of thymidine O2 atoms on the complementary strand; the fixed geometry of the cyclopropane linker forces the position of the netropsin moieties closer to 5′AAAA strand segments in (1*S*,2*S*)-BNC as opposed to the 5′-TTTT segments in the case of (1*R*,2*R*)-BNC.

Relative Stabilities of Diastereomeric Complexes. Relative comparison of the DNA binding affinities of (1*R*,2*R*)- and (1*S*,2*S*)-BNC to observe enantiomeric discrimination was also obtained from the thermal denaturation temperature measurements. From the temperature-variable NMR experiments, the helix-coil transition was determined to be 65 and 52 °C, respectively, for (1*R*,2*R*)- and (1*S*,2*S*)-BNC:d(CGAAAATTTTCG)$_2$ complexes. Under the same low salt and identical DNA concentration conditions the helix-coil transition of the free DNA alone occurs at 38 °C. The corresponding ΔT_m values of 27 and 14 °C, respectively, for the dodecamer complexes of (1*R*,2*R*)- and (1*S*,2*S*)-BNC indicate a relatively stronger binding of (1*R*,2*R*)-BNC with this sequence.

A comparison of the binding affinities was also obtained by monitoring optical absorbance changes at 260 nm during thermal denaturation of the complexes formed between (1*R*,2*R*)- and (1*S*,2*S*)-BNC and two different synthetic duplex DNA polymers, the homopolymer poly(dA)·poly(dT) and the alternating copolymer poly[d(A-T)]·poly[d(A-T)]. The ΔT_m values (Figure S4, supplementary material) were obtained at varying ligand to DNA ratios. Comparison of the ΔT_m values shown in Table T2 (supplementary material) illustrates the high affinity of both the ligands for double helical DNA and the observation of a monophasic denaturation behavior even at low ligand to DNA ratios suggests a single bidentate mode of interactions between the two netropsin subunits and DNA. Although (1*R*,2*R*)-BNC shows a higher affinity than the enantiomeric (1*S*,2*S*)-BNC toward both kinds of polymer sequences, any correlations between structural and thermodynamic data must await a complete thermodynamic profile for the DNA binding of these ligands especially in terms of relative enthalpy/entropy contributions from specific ligand–DNA interactions.[15a,b]

Restrained Molecular Modeling. Semiquantitative modeling of the diastereomeric complexes was carried out using the AMBER molecular mechanics package. The intermolecular contacts listed in Table 3 were used as constraints. The most favored solution structures of the DNA complexes with (1*R*,2*R*)- and (1*S*,2*S*)-BNC that are obtained from the energy-minimization procedures are shown in Figures 7 (parts a and b, respectively). For comparisons, the experimental NOE distance constraints and refined distances obtained from the final models are provided in the supplementary material (Tables T3 and T4). Also listed therein are the putative intermolecular hydrogen bonds (Tables T5 and T6) that are most likely to form on the basis of measured donor–acceptor distances from these models. The inspection of the hydrogen-bond networks shows that such interactions with thymidine O2 atoms of DNA are stronger and more favorable in the (1*R*,2*R*)-BNC:DNA complex compared with the (1*S*,2*S*)-BNC:DNA complex. Energy calculations (Table T7, supplementary material) show an overall difference of 5.2 kcal·mol^{-1} between the two complexes, which presumably arises from a differential contribution equivalent to two hydrogen bonds. The two complexes show the occupancy of the DNA minor groove at $(A_4T_4)_2$ sites by the extended ligand structures without significant distortions of the double helix. Consistent with the NMR data and in particular the intermolecular ligand–DNA NOE interactions emanating from the "outside" face of (1*S*,2*S*)-BNC, a

(29) Blasko, A.; Browne, K. A.; He, G.-X.; Bruice, T. C. *J. Am. Chem. Soc.* **1993**, *115*, 7080–7092.

Table 3. Intermolecular NOE Contacts, Experimentally Observed in the 2D-NOESY Spectra, in the Case of Two (BNC-DNA) Complexes

ligand protons	DNA protons	cross peak no.
(a) (1*R*,2*R*)-BNC[a]		
C3 H	A6 H2	1
	A5 H2	2
	A6 H1′, T8 H1′	3
	T7 H1′	4
C9 H	A4 H2	5
	T9 H1′	6
C14 H	A3 H2	
C15 H	A3 H2	
C17 H	G2 H1′	
	C11 H1′	
	C11 H2′	
(b) (1S,2S)-BNC[b]		
C3 H	A6 H2	1
	A5 H2	2
	A6 H1′, T8 H1′	3
	T7 H1′	4
C5 H	A6 H2	5
C9 H	A4 H2	6
	A3 H2	7
	A5 H1′	8
	T9 H1′	9
C11 H	A4 H2	10
	A5 H1′	11
	T8 H1′	12
C14 H	A3 H2	
C15 H	A3 H2	
C17 H	G2 H1′	
	C11 H1′	

[a] See Figure 4 for peak numbers. [b] See Figure 6 for peak numbers.

significant change can be seen in the dihedral angles between adjacent pyrrole rings (Table T7, supplementary material).

Discussion

DNA minor groove binding ligands such as netropsin and distamycin owe their high-affinity and sequence selective recognition characteristics to an ensemble of hydrogen-bond forming amide NH groups, positively charged end groups for electrostatic stability, and orthogonally placed planar pyrrole rings to provide favorable van der Waals interactions.[3,5,6] The regularly spaced disposition of these groups creates a structural complementarity between the crescent shape of the ligands and the natural curvature of the DNA helix. Our interest, and that of others, in designing longer netropsin/distamycin analogs stems from the general prediction that recognition of larger binding site sizes would lead to higher sequence specificity toward DNA[8,10-12] and that minor groove binders capable of binding to a unique site sequence of 14–16 base pairs in the human genome should find applications as gene control agents.[2f] A simple extension of the *N*-methylpyrrolecarboxamide framework for this purpose suffers from the lack of synchronous isohelical contacts due to an apparent mismatch between the pyrrolecarboxamide repeat units and adjacent DNA base pairs.[8,9] One significant advantage of linking two netropsin/distamycin subunits is the spacer-assisted convergence of useful functional groups, particularly the periodically spaced amide NH groups, which permits a greater number of hydrogen-bonding interactions with AT base pairs along an extended length of the DNA minor groove.

This study demonstrates the use of controlling absolute configuration of a geometrically constrained linker group in the design of dimeric ligands which favorably exploit the molecular interactions that have been shown to contribute toward specific molecular recognition and efficient binding between the neotropsin and distamycin molecules and DNA. The structural details on the DNA minor groove binding, obtained for the first time on such dimeric netropsin molecules, expand our study on the influence of linker geometry on the efficiency of bidentate binding modes[10c] for these compounds designed to extend the code for an isohelical and chiral recognition of longer AT base pair sites through the minor groove. These structures, with their relatively few degrees of rotational freedom, also provide more attractive frameworks than the conformationally flexible linker chains of methylene groups.[10b,c]

The present results from 2D NMR spectroscopy and restrained molecular modeling methods have helped elucidate the DNA minor groove binding characteristics of the enantiomeric bis-netropsin ligands. The exchangeable and nonexchangeable protons in the NMR spectra of a DNA fragment, d-(CGAA-AATTTTCG)$_2$, and of the two diastereomeric ligand–DNA complexes were assigned by analysis of the phase-sensitive NOESY spectra using the standard methods of delineating sequential connectivity pathways.[23]

The ligand-free DNA was confirmed to be a right-handed B-type from characteristic NOE patterns and exhibits features that relate to its "bending" properties which are evident from characteristically anomalous NOE intensities.[25] Significantly intense cross peaks were associated with *inter*strand NOE interactions between the adenine H2 (*i* residues) and sugar H1′ protons ($j+1$ residues) on the complementary strand suggesting that the corresponding distance estimates are close to ~0.35 nm and that the minor groove formed at these segments is narrowed to ~0.90–0.95 nm (*viz.* across the strand phosphate-to-phosphate distances in a base-pair). Also, such compression of the minor groove appears more pronounced at the central A_5·T_8 and A_6·T_7 base pairs of the sequence, presumably due to the 5′-AT step at the center, since intermediate characteristics (interstrand AH2-H1′ distances of ~0.4 nm) are exhibited by the A_3·T_{10} and A_4·T_9 base pairs.

Minor groove binding of (1*R*,2*R*)- and (1*S*,2*S*)-BNC to the dodecameric DNA duplex was characterized as a single symmetric type in each instance, where the C_2-symmetry of DNA and that of the ligands is maintained. Judging by the lack of any complexation-induced asymmetry, in the form of doubling of DNA or ligand proton resonances, it is evident that minor groove binding of two netropsin-like fragments in both (1*R*,2*R*)- and (1*S*,2*S*)-BNC occurs in a cooperative bidentate fashion. Monodentate binding of individual netropsin fragments to any of the five potential 4 base pair long AT sites in d(CGAAAATTTTCG)$_2$ would be expected to have an orientational preference, as observed for netropsin and distamycin,[5,6,30] which must manifest in a removal of the degeneracy in the palindromic dodecanucleotide sequence. The twofold C_2 symmetry of both the DNA duplex and the ligands in the complexes was retained over the entire temperature range (5–50 °C) which excludes the arguments for a rapid exchange of monodentate associated netropsin subunits between two equivalent binding sites.

Binding within the minor groove of the duplex DNA dodecamer is evident from numerous intermolecular NOE contacts between the ligand protons and the H2 protons of adenine residues that are accessible for interactions only through the minor groove (Table 3; Figure 5). Complementary evidence for such binding mode is provided by the greater complexation-induced chemical shift changes for selected H2/H1′/H2′/H2″ protons positioned in the DNA minor groove compared to the aromatic base and thymidine CH3 protons lying in the major groove (Figures S5 and S6, supplmentary material). Both (1*R*,2*R*)- and (1*S*,2*S*)-BNC ligands bind without causing major distortions in the DNA (Figure 7a,b), and in both cases the only perturbations of the DNA double helical conformation observed as a result of ligand binding are limited to an expansion or widening of the minor groove which were characterized by a loss of the NOE cross peaks ascribed in the free DNA duplex to the *inter*strand interactions between the adenine H2 protons (on *i*th residues) and sugar H1′ protons (on $j+1$ residues). Minor groove binding ligands in general exploit the plasticity associated with DNA and give rise to such an increase in the DNA groove width.

The most striking feature which illustrates the differences in the torsional flexibility of the DNA-bound ligands despite similar

geometries for the cyclopropane linker is the observation of specific intermolecular NOE interactions, only in the case of (1*S*,2*S*)-BNC, between the ligand protons lining both the concave and convex faces (H3/H9 and H5/H11, respectively) and adenine-H2 protons at the floor of the DNA minor groove, as schematically represented in Figure 5b. This mirrors the degree of rotational freedom around linkages between *N*-methylpyrrole rings in the adaptability of the netropsin and distamycin molecules in binding to DNA. A preferentially higher degree of twists in the individual elements in (1*S*,2*S*)-BNC compared with that for (1*R*,2*R*)-BNC may be attributed to a strand-specific alignment of the netropsin fragments away from the TTTT arrangement. The movement of amide NHs toward thymidine O2 atoms to form effective hydrogen-bonds therefore induces a counterclockwise twist of the *N*-methylpyrrole rings, presumably due to disfavorable steric interactions between the amide carbonyl oxygens and *N*-methyl groups on pyrrole rings. Strand-specific association of monomeric netropsin and distamycin molecules has also been observed previously in solution NMR studies of their DNA complexes,[30,31] albeit without such direct differentiating evidence as obtained here in the case of BNC ligands.

The cyclopropane linker with its dicarboxamide substituents in a *trans* configuration is similar to a *trans*-olefinic tether, and they closely mimic the DNA minor groove directed convergence and separation of amide NHs in the *N*-methylpyrrolecarboxamide repeat units (Figure 1c).[1a,e] Such compatibility of the *trans*-cyclopropanedicarboxamide with the DNA minor groove, together with the overall structural complementarity between the extended ligands and the curvature of DNA, contributes to an effective bidentate binding spanning 8 AT base pairs. The model representations (Figure 5) for both (1*R*,2*R*)- and (1*S*,2*S*)-BNC in their complexed forms illustrate identical geometries for the central cyclopropane tether, with regard to the C3′-methylene group, that are shown to be projected away from the DNA minor groove. This is consistent with the similar trends in the complexation-induced chemical shift differences for the ligand protons in the two cases (Figure S7), and the absence of NOE interactions involving the methylene protons of cyclopropane and any of the DNA protons in either case. Alternative orientations with the cyclopropane methylene group pointing inwards and facing the minor groove (Figure 8) are presumably disfavored owing to severe steric interactions. In addition, such an orientation for (1*S*,2*S*)-BNC, for example, would be expected to exhibit only a localized structural perturbation in the immediate vicinity of the cyclopropane template rather than such distinct structural changes as observed over the entire length of the individual netropsin subunits.

The high degree of cooperativity and increased stability observed with the bis-netropsin derived from linker (1*R*,2*R*)-BNC are likely due, in part, to entropic considerations. Figure 9a shows how the relative arrangement of two netropsin subunits in this absolute configuration is highly preorganized for a strand-selective binding so that when one of the subunits of the dimer binds to the target 5′-TTTT site, the other subunit is located in close proximity for binding to the same target site on the opposite strand. Importantly, the DNA recognition properties associated with the minor groove binding netropsin subunits are also preserved in the binding of (1*S*,2*S*)-BNC. The altered ligand conformation (Figure 9b), differing only in the handedness of the central cyclopropane linker, binds differently along the minor groove of DNA resulting from a predisposed orientation of the netropsin subunits along 5′-AAAA sites which is not conducive to forming effective hydrogen bonds.

In the model representations illustrated in Figure 5, it is important to note the lack of the twisting of amide groups and pyrrole rings in the case of (1*R*,2*R*)-BNC which appears to result from a colinear arrangement of the two netropsin arms along the DNA 5′-AAAATTTT segment and preoriented with a bias for the strands containing TTTT stretch. In the case of (1*S*,2*S*)-BNC, however, the netropsin arms are predisposed away from the strands containing the TTTT stretches such that, in order to facilitate hydrogen-bonding between the amide NHs of the netropsin subunits and the thymidine O2 atoms, the former planar groups must twist, with an accompanying twist of the pyrrole rings. Kopka *et al.* have previously proposed a steric clash between amide NH and pyrrole CH groups as one possible source of the torsional flexibility of the amide-pyrrole linkages.[6b-d] On the contrary, we favor a mechanism accounting for the origins of

(a) (1*R*,2*R*,)·BNC·d(CGAAAATTTTCG)$_2$

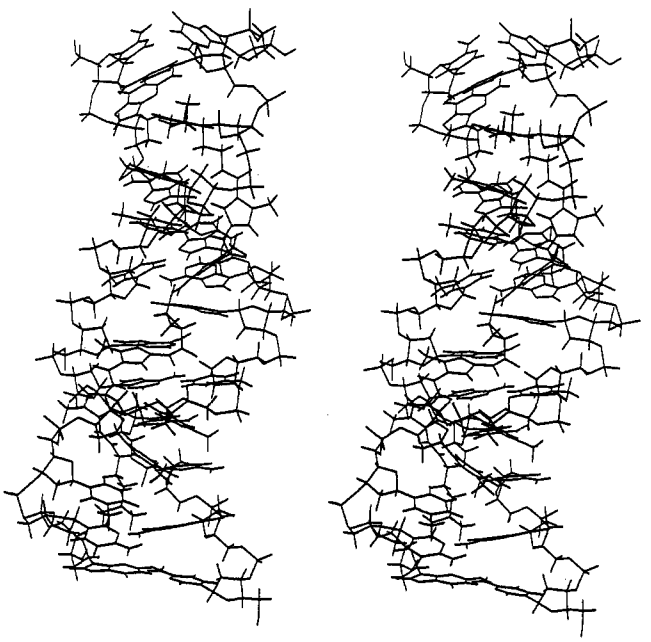

(b) (1*S*,2*S*)·BNC·d(CGAAAATTTTCG)$_2$

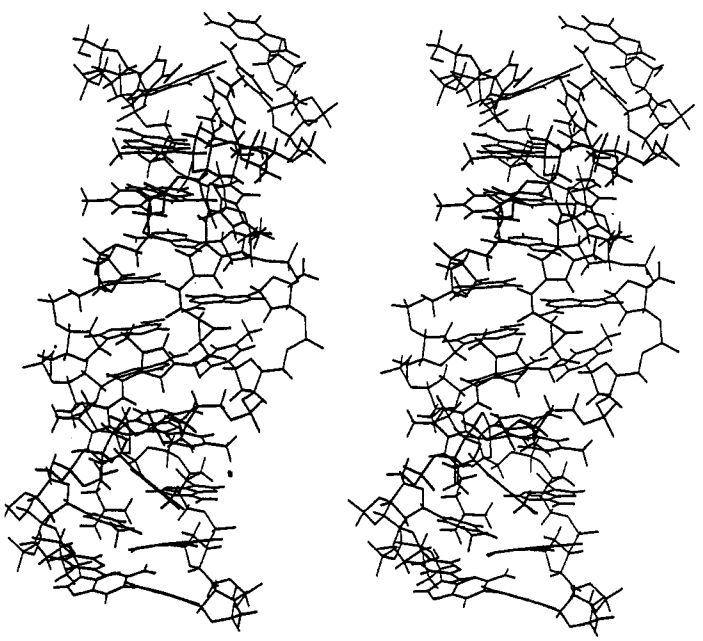

Figure 7. Stereoviews of the three-dimensional model structures for the dodecamer duplex DNA complexes with (a) (1*R*,2*R*)-BNC and (b) (1*S*,2*S*)-BNC ligands, obtained by energy refinement with semiquantitative NOE distance constraints.

(30) Pelton, J. G.; Wemmer, D. E. *J. Biomol. Struct. Dyn.* **1990**, *8*, 81–97.
(31) Sarma, M. H.; Gupta, G.; Sarma, R. H. *J. Biomol. Struct. Dyn.* **1985**, *3*, 433–436.

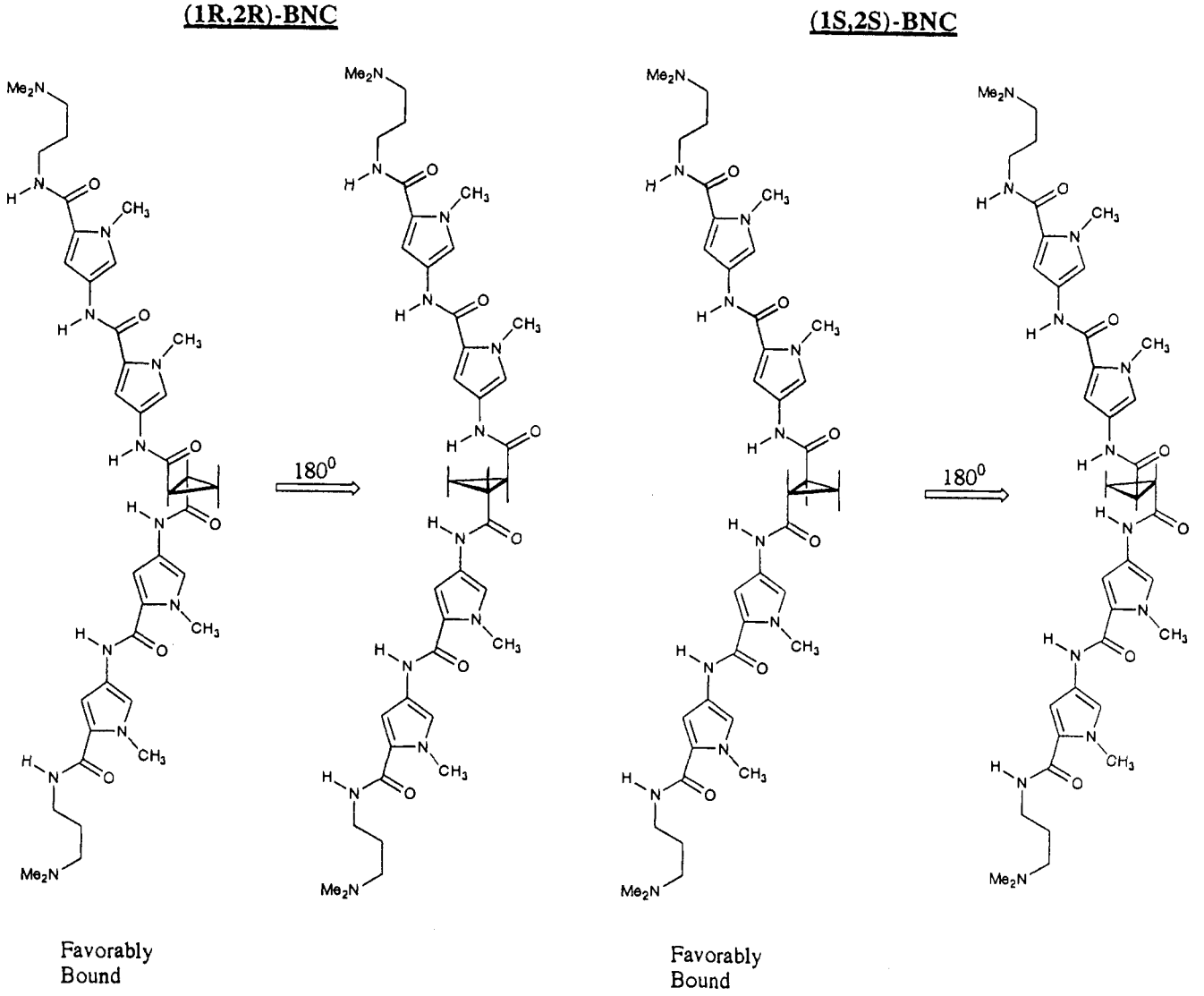

Figure 8. Alternative orientations of (1*R*,2*R*)-BNC and (1*S*,2*S*)-BNC, each shown in the right- and left-handed cyclopropane configuration related to each other by a 180° rotation, with the evident C_2-symmetry. The structures in the experimentally observed DNA-bound states are marked as "favorably bound".

such twists in the form of the following mutually exclusive effects (Figure 5b): (a) a twist in the planar amide groups (angles depicted as ψ_1, ψ_3, and ψ_5), which would bring the amide carbonyl oxygen and *N*-methyl groups too close in an already disfavorable syn position and force a twist in the pyrrole rings around the N–C–C–O bonds (angles depicted as ψ_2 and ψ_4) and/or (b) a repulsive van der Waals interaction of the orthogonal pyrrole rings with the sugar-phosphate backbone forming the walls of the minor groove at 5′-AAAA stretches. Note that twisting around ψ_6 cannot be resolved from the present data or is presumably absent due to the fact that the oxygen atom of the amide carbonyl C1=O1 *does not* suffer from a severe repulsive steric clash with the C3′–H bond in cyclopropane (in contrast with *N*-Me bonds for ψ_2 and ψ_4). The most favored solution structures from NOE—distance-dependent restrained molecular modeling (Figure 7a,b)—show that the deviation from coplanarity of the adjacent pyrrole rings is greater for (1*S*,2*S*)-BNC:DNA complex than for the (1*R*,2*R*)-BNC counterpart (Table T7, supplementary material).

We speculate that additional experiments with an alternative DNA fragment, d(CGTTTTAAAACG)$_2$, should provide an absolute proof for such binding-induced twisting features; a mirror-image picture should emerge from such experiments, i.e., a twisting of individual planar units in the case of (1*R*,2*R*)-BNC, and not in the case of (1*S*,2*S*)-BNC; assuming that in the bound state, the cyclopropane linker in all these cases adopts the same configuration (with the methylene group projecting away from the minor groove of DNA).

Although a general consensus exists from the NMR and X-ray crystal structures of DNA–netropsin/distamycin complexes[5,6] on the overall structural complementarity between these minor groove binding ligands and the curvature of DNA, two important questions on the (a) role, types, and number of hydrogen bonds and (b) the source of conformational adaptability in terms of the dihedral angles between successive planar elements of the ligands remain open. The observed diversity in ligand conformations in the crystalline state may arise from the sequence context of the DNA fragments chosen for these studies or from a selection by crystal-packing forces. A survey of the available structures of netropsin–DNA complexes[6] shows that the netropsin molecule is able to bind symmetrically across the two strands in an optimized position at the centrally located four base pairs in heteronomous AT sites consisting of (AATT)$_2$, (ATAT)$_2$, and (AAATTT)$_2$, and it remains unclear whether the ligand molecules could by asymmetrically positioned against a poly(dA) or a poly(dT) strand.[31] In this context, it is important to note that such sequences consisting of uninterrupted stretches of poly(dA)·poly(dT) are preferred for binding of netropsin over those containing alternating A·T and T·A base pairs.[3,15a,b] A recent analysis also indicates that within the 4–5 base pair long AT-rich binding sites for the tris(*N*-methylpyrrolecarboxamide) framework of distamycin, the sequence preferences rank in the order of decreasing affinity 5′-

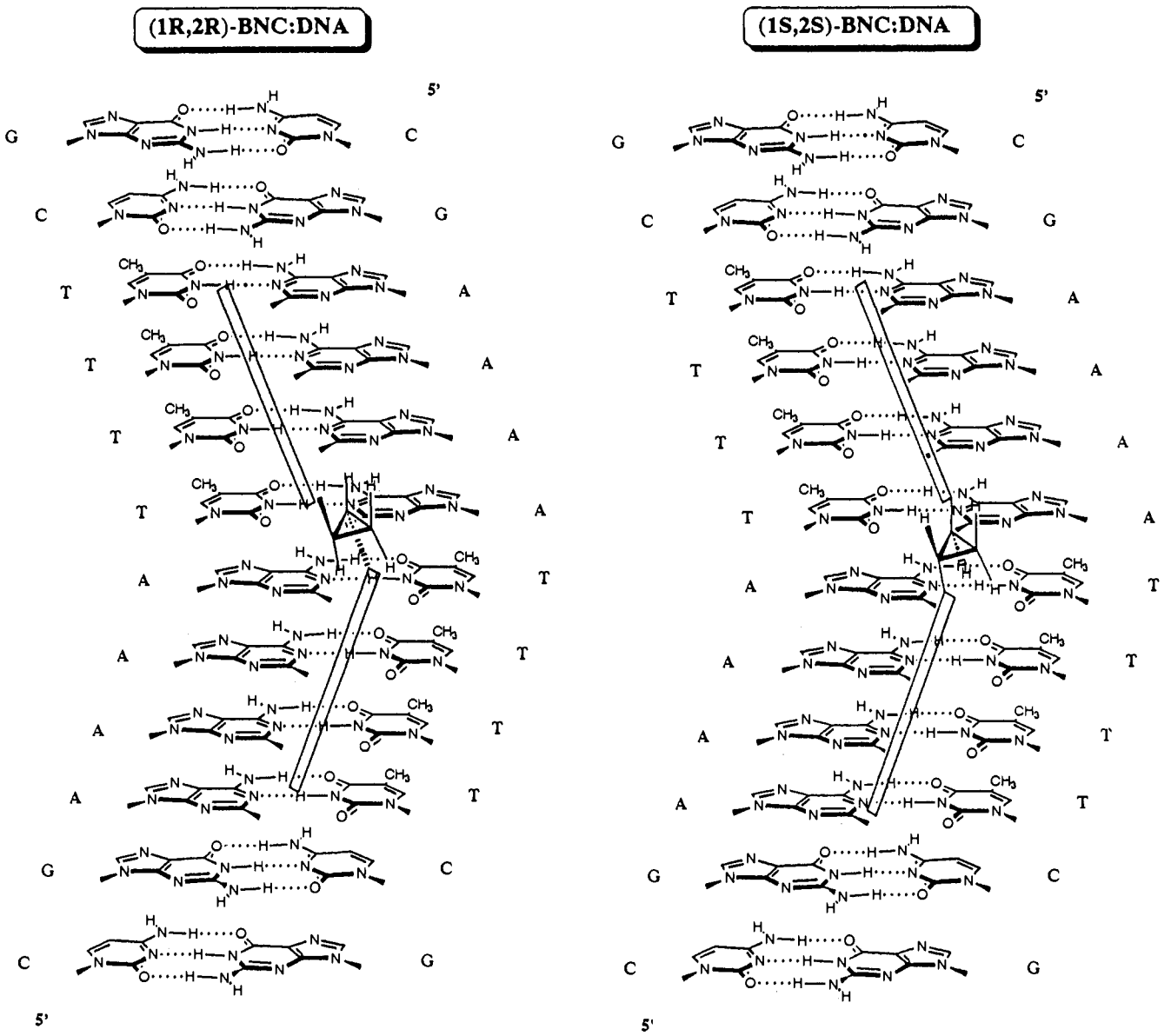

Figure 9. Model representations for the isohelical bidentate mode of binding with a sequence- and strand-specificity as experimentally observed for 1:1 complexes of d-(CGAAAATTTTCG)$_2$ with (1*R*,2*R*)-BNC and with (1*S*,2*S*)-BNC. The proximity and relative orientations of the two ligands, relative to the minor groove of the DNA fragment is shown for (a) (1*R*,2*R*)-BNC and (b) (1*S*,2*S*)-BNC. Two netropsin arms in a C_2-symmetry arrangement are shown by long bars, and the alignment of these units against the strands containing 5'-TTTT and 5'-AAAA segments, respectively, is evident due to the chirality of the cyclopropane linker.

TTTTT-3' > 5'-AATAA-3' > 5'-TTAAT-3' as determined by quantitative footprinting data on a pBR322 DNA fragment.[15c,d]

In the present study, we are able to constrain individual netropsin-like fragments in a stereochemically controlled environment so that for (1*R*,2*R*)-BNC these units are asymmetrically fixed along the TTTT-stretch, and conversely for (1*S*,2*S*)-BNC an AAAA-stretch is offered for interactions with the netropsin units. The results show that only in the case of (1*S*,2*S*)-BNC, interactions with DNA lead to a significant twist in the successive *N*-methypyrrole ring and amide linkages. Asymmetric association of the netropsin units with a (dA)$_4$ stretch is therefore far less optimum than the corresponding binding to a (dT)$_4$ segment, which may arise from an inherent likeness of oligo(*N*-methylpyrrolecarboxamide)s to form single linear hydrogen bonds between the amide NHs and the thymidine O2 atoms rather than a specific binding of netropsin being created by three-center bifurcated hydrogen bonds between NH groups of peptide linkages of the ligand and O2 and N3 atoms of thymidine and adenosine residues, respectively.

Alternatively, another possible explanation which we cannot distinctly differentiate from the NMR results is that strand-specific van der Waals contacts between the netropsin backbone atoms and the sugar-phosphate backbone forming the walls of the minor groove may not permit an asymmetric association of the (1*S*,2*S*)-BNC ligand along the AAAA segments. A further distinction between the two proposals should be possible from a X-ray crystal structure, for example, of a netropsin complex with an asymmetrical DNA duplex, d[CGCAAAAAAGCG]·d-[CGCTTTTTTGCG].

General Implications and Comparisons of the Covalently Linked End-to-End with the Side-by-Side Dimeric Motifs. The preparation and the DNA minor groove binding characteristics of such bis-netropsin/distamycin ligands as described here has important implications in the design of extended peptide analogs capable of tightly binding longer sequences with high specificities. Thus, the use of a rigid stereochemically defined cycloalkane template to link together two netropsin like fragments is particularly significant to achieve an end-to-end bidentate association of the dimeric ligands with DNA in a strand-selective fashion by creating an almost perfect one-to-one correspondence between the DNA base pairs and the pyrrolecarboxamide units along the complete length of the ligands. Simple addition of two molar equivalents

of shorter di- and tripyrrolecarboxamide units (netropsin and distamycin respectively), to saturate the adjacently arranged AAAA and TTTT sites would be complicated by the formation of antiparallel side-by-side dimers as shown by Wemmer and co-workers in the case of a distamycin/A_3T_3 complex[33] and confirmed by us for complexes of the A_4T_4 sites with distamycin-A and distamycin-2 containing the bis(*N*-methylpyrrolecarboxamide) framework of BNC ligands described above.[34] The use of a covalent linker element between two netropsin/distamycin units obviates such complications. The rigidity of linker is also desirable to overcome possible formation of fold-back side-by-side dimeric motifs predicted in the case of simple polymethylene linked bis-netropsins. The stereochemically defined cyclopropane linker should also find a general application in designing dimeric minor groove binding ligands for the specific binding modes of an end-to-end type for targeting long DNA sequences selectively by combining the latest generation of lexitropsins that were prepared for mixed AT/GC sequence specificities and which exhibit either homo- or heterodimeric side-by-side binding motifs.[35]

To our knowledge there is only one other example of a stereochemical control of bidentate modes of minor groove binding agents, and this was reported for dihydroxysuccinamide linked bis-netropsins.[14] However, the relatively higher concentrations of (*R*,*R*) and (*S*,*S*) forms required, compared to that of an achiral succinamide analogue, to produce equal intensity footprints on a DNA fragment showed an attenuated binding affinity owing to a markedly increased steric bulk of the chiral tetrahedral centers containing the OH groups.

Conclusions

The principal conclusions we draw from the present study are as follows: (i) both (1*R*,2*R*)- and (1*S*,2*S*)-BNC bind to DNA by a single binding mode which is characterized as a bidentate association of the netropsin subunits; (ii) the minor groove binding, the binding location, and site size of 8-base pair long (AAAATTTT)$_2$ segment is the same for both the enantiomers which differ only in the handedness of the central cyclopropane linker; (iii) the structural details for the binding mode show distinct differences, in the adaptability of the enantiomeric ligands for binding to the same site, that are reflected in the nature of intermolecular NOE interactions between the ligands and DNA; (iv) the (1*R*,2*R*)-form is better suited for interaction with the 5′-AAAATTTT-3′ sequence; (v) the source of enantiomeric discrimination is presumably the patterns of hydrogen bonds in a strand-specific association with contiguous thymine residues; and (vi) directionality in binding can be controlled by the stereochemistry of the linker group in the design and development of minor groove binding ligands for longer DNA targets.

Acknowledgment. Synthesis of DNA was carried out at the laboratories in Calgary (R.T.P.). J.G. is acknowledged for preliminary work on the synthesis of ligands. The financial support for this work was provided by the Natural Sciences and Engineering Research Council of Canada, and the Canadian Medical Research Council (to J.W.L), and by a Centers of Excellence Grant HHS-2-D3400006-07 (to G.C.H).

Supplementary Material Available: Three figures (S1, S2, and S3) showing the contour plots of phase-sensitive 2D-NOESY spectra of duplex d(CGAAAATTTTCG)$_2$, along with the expanded subsections showing the cross peaks between the purine/pyrimidine base protons and H2′/H2″/T-Me protons, and those showing the cross peaks observed between the exchangeable imino protons and adenine H2 protons in a NOESY spectrum of the duplex in 90% H_2O–D_2O; Figure S4, first-order differential melting curves ($\Delta OD/\Delta t$ versus t) for the helix-to-coil transitions of (a) poly(dA)·poly(dT) and (b) poly(dA·dT)·poly(dA·dT) and in the presence of (1*R*,2*R*)- or (1*S*,2*S*)-BNC ligands; Figures S5 and S6, complexation-induced chemical shift differences for selected DNA protons, in the 1:1 complexes of (1*R*,2*R*)- and (1*S*,2*S*)-BNC with d(CGAAAATTTTCG)$_2$; Figure S7, plots of chemical shift differences observed for the (1*R*,2*R*)- and (1*S*,2*S*)-BNC ligands upon interaction with the DNA duplex. Table T1, complexation induced chemical shift differences for selected DNA protons in the 1:1 ligand–DNA complexes; Table T2, ΔT_m values determined for the complexation of (1*R*,2*R*)- and (1*S*,2*S*)-BNC ligands to the nonalternating DNA copolymer poly(dA)·poly(dT) and the alternating [poly(dA·dT)] polynucleotide; Tables T3 and T4, experimental NOE distance estimates used as restraints in molecular modeling of the complexes of d(CGAAAATTTTCG)$_2$ with (1*R*,2*R*)- and (1*S*,2*S*)-BNC and refined distances obtained from the final energy minimized models; Tables T5 and T6, putative hydrogen bonds most likely to form on the basis of interproton distances measured from the energy minimized model structures for the complexes with (1*R*,2*R*)-BNC and (1*S*,2*S*)-BNC; Table T7, energy calculations and measurements of dihedral angles ψ_1–ψ_6 defined in the manuscript for the refined structures of the duplex d(CGAAAATTTTCG)$_2$ and the complexes with (1*R*,2*R*)- and (1*S*,2*S*)-BNC (15 pages). This material is contained in many libraries on microfiche, immediately follows this article in the microfilm version of the journal, and can also be ordered directly from ACS; see any current masthead page for ordering information.

(32) A conceptually similar model of linking two all-T oligodeoxyribonucleotide strands by an achiral xylolyl group (a "switchback" template) has been developed for targeting long self-complementary AT sites via triplex formation, on the basis of the known preference of the added Ts for A-residues of TAT triads through the major groove. (a) Riordon, M. L.; Martin, J. C. *Nature (London)* **1991**, *350*, 442–443. (b) McCurdy, S.; Moulds, C.; Froehler, B. C. *Nucleosides Nucleotides* **1991**, *10*, 287–290. (c) Froehler, B. C.; Terhorst, T.; Shaw, J.-P.; McCurdy, S. N. *Biochemistry* **1992**, *31*, 1603–1609.

(33) (a) Pelton, J. G.; Wemmer, D. E. *Proc. Natl. Acad. Sci. U.S.A.* **1989**, *86*, 5723–5727. (b) Pelton, J. G.; Wemmer, D. E. *J. Am. Chem. Soc.* **1990**, *112*, 1393–1399. (c) Wemmer, D. E.; Fagan, P.; Pelton, J. G. In *Molecular Basis of Specificity in Nucleic Acid-Drug Interactions*; Pullman, B., Jortner, J., Eds.; Kluwer Acad. Publishers: Dordrecht, Netherlands, 1990; pp 95–101. (d) Fagan, P. E.; Wemmer, D. E. *J. Am. Chem. Soc.* **1992**, *114*, 1080–1081.

(34) Singh, M. P.; Lown, J. W., manuscript in preparation.

(35) (a) Dwyer, T. J.; Geierstanger, B. H.; Bathini, Y.; Lown, J. W.; Wemmer, D. E. *J. Am. Chem. Soc.* **1992**, *114*, 5911–5919. (b) Mrksich, M.; Wade, W. S.; Dwyer, T. J.; Geierstanger, B. H.; Wemmer, D. E.; Dervan, P. B. *Proc. Natl. Acad. Sci. U.S.A.* **1992**, *89*, 7586–7590. (c) Geierstanger, B. H.; Dwyer, T. J.; Bathini, Y.; Lown, J. W.; Wemmer, D. E. *J. Am. Chem. Soc.* **1993**, *115*, 4474–4482. (d) Mrksich, M.; Dervan, P. B. *J. Am. Chem. Soc.* **1993**, *115*, 2572–2576. (e) Dwyer, T. J.; Geierstanger, B. H.; Mrksich, M.; Dervan, P. B.; Wemmer, D. E. *J. Am. Chem. Soc.* **1993**, *115*, 9900–9906.